# Triazolyl Donor/Acceptor Chromophore Decorated Unnatural Nucleosides and Oligonucleotides with Duplex Stability Comparable to That of a Natural Adenine/Thymine Pair

Subhendu Sekhar Bag,*,[†] Sangita Talukdar,[†] Katsuhiko Matsumoto,[‡] and Rajen Kundu[†]

[†]Bio-organic Chemistry Laboratory, Department of Chemistry, Indian Institute of Technology, Guwahati-781039, India
[‡]Institute of Advanced Energy, Kyoto University, Uji, Kyoto 611-0011, Japan

S *Supporting Information*

R = Protective groups; Ac = Acceptor Unit; Do = Donor Unit; UNN = Unnatural (UN) Nucleoside
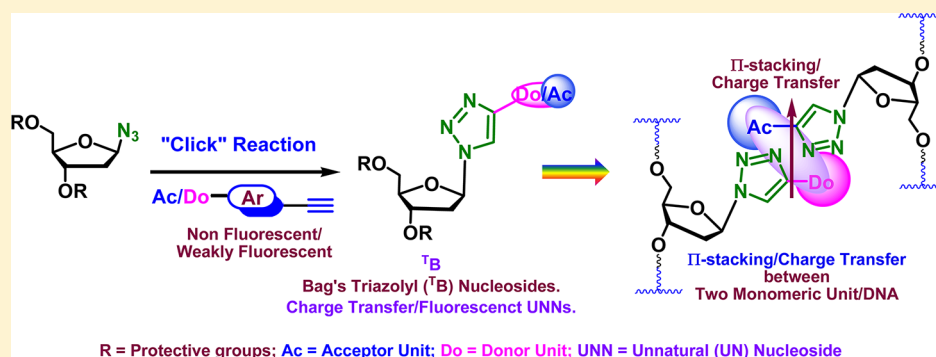
ABSTRACT: We report the design and synthesis of triazolyl donor/acceptor unnatural nucleosides via click chemistry and studies on the duplex stabilization of DNA containing two such new nucleosides. The observed duplex stabilization among the self-pair/heteropair has been found to be comparable to that of a natural A/T pair. Our observations on the comparable duplex stabilization has been explained on the basis of possible $\pi-\pi$ stacking and/or charge transfer interactions between the pairing partners. The evidence of ground-state charge transfer complexation came from the UV−vis spectra and the static quenching of fluorescence in a heteropair. We have also exploited one of our unnatural DNAs in stabilizing abasic DNA.
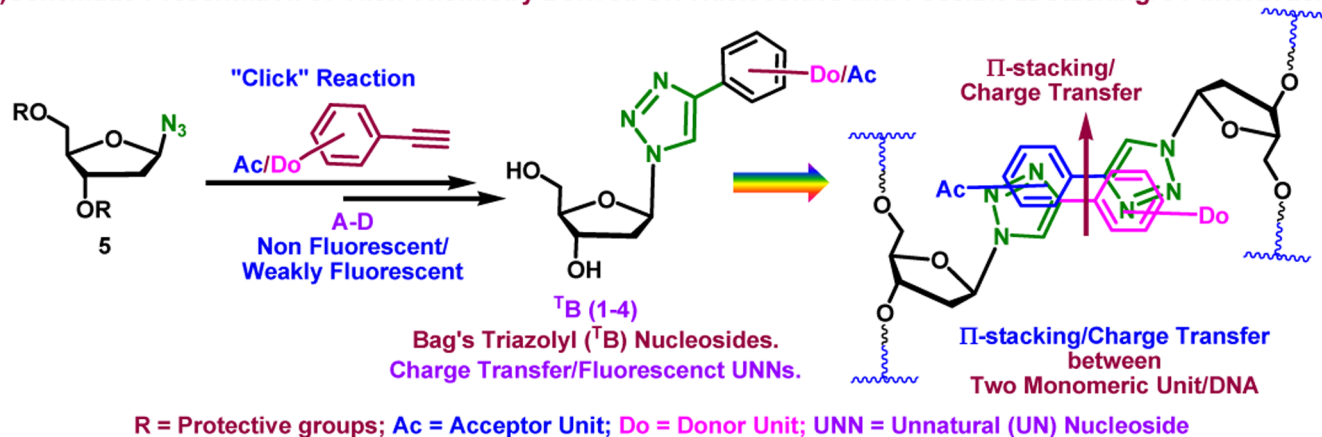
INTRODUCTION

The design and synthesis of nonnatural analogues of nucleosides for the replacement of the natural nucleobases have attracted much research interest in recent years.[1] Toward this journey, a large number of non-natural nucleosides capable of showing π-stacking interaction properties have been developed, and their biophysical properties in the context of DNA have vigorously been investigated. For example, a number of base analogues with orthogonal H-bonding complementarities[2] in relation to the natural Watson−Crick H-bonding have been exploited to examine the importance of hydrogen-bonding interactions in the stabilization of nucleic acid structure, in the study of interbiomolecular interactions,[3a,b] and in the base recognition ability of enzymes.[3c−g] Several modified nucleosides with reporter functionalities have also been synthesized for monitoring the local microenvironmental change around the nucleic acids associated with interbiomolecular interactions.[4] Creation of non-H-bonding unnatural nucleobase surrogates by Kool et al. has opened a new dimension in the design of hydrophobic unnatural DNA base analogues.[5] Thus, they have explored the possible aromatic stacking, hydrophobic, or CH−π interactions between the bases and shown that these attractive forces are good enough to stabilize a DNA duplex and are well recognized by DNA polymerases. Triggered by Kool's

work, much effort has been put forth to develop non-natural, stable, hydrophobic base pairs of orthogonal recognition properties toward expanding the genetic alphabet.[5] Recently, the design of unnatural DNA base pairs with tuned charge transfer/photophysical properties has been a rapidly growing research field toward the development of nucleic acid based diagnostics and sensing materials.[6] While the development of bases with improved charge transfer characteristics would lead to oligonucleotides with novel electronic properties,[6] the fluorescent nucleobases could offer an opportunity for in vivo imaging as well as for the development of nucleic acid based sensors.[7] Toward this end, several unnatural nucleobases have appeared in the literature for the development of functional nucleic acids.[4g,8] However, the rational design of non-hydrogen-bonding base pairs remains a challenge. In most of the design of non-hydrogen-bonding base pairs, researchers have concentrated mainly on factors such as π-stacking, hydrophobicity, steric shape mimicry, and in a few cases the dipole moment, etc. in the stabilization of the DNA duplex.[5]

Cu(I)-catalyzed azide−alkyne cycloaddition reaction[9a] has drawn attention only in recent years in the field of nucleic acid
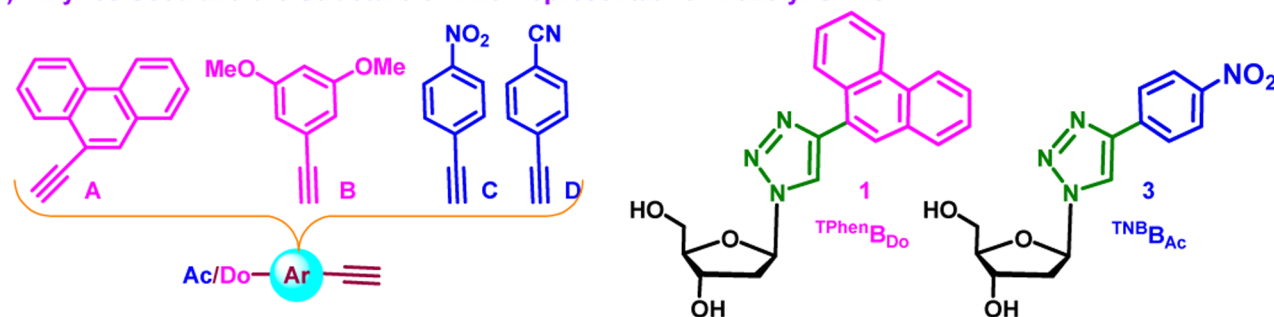
Figure 1. (I) Schematic presentation of conceptual duplex stabilization with triazolyl unnatural nucleosides (UNNs). (II) Alkynes used in this study and the structures of nucleosides incorporated into DNA.

chemistry for the design of functional nucleic acids of potential value in biology, medicine, material sciences, and nano-technology.[9] However, donor and/or acceptor aromatic linked click triazoles as unnatural nucleobase surrogates have not been explored.[10] To date, in the development of unnatural bases, the charge transfer interaction among the heteropair has not been considered. As a part of our ongoing research effort toward generation of molecules with tuned photophysical properties via click reaction,[11] we thought that it would be worthwhile to synthesize triazolyl nucleosides containing donor/acceptor aromatics to produce a modulated photophysical response in the unnatural nucleosides (UNNs). Therefore, we disclose, herein, our conceptual design and synthesis of triazolyl donor/acceptor unnatural nucleosides derived from azide−alkyne cycloaddition reaction with interesting photophysical properties and the capability of showing π-stacking as well as a charge transfer characteristic feature among themselves and the oligonucleotides containing two of our modified triazolyl nucleosides (TB's) (Figure 1).

The Concept. The logic behind our choice of triazole linked with donor/acceptor aromatics to be the nucleobases is as follows: (a) Triazoles are metabolically inert. (b) The triazole units are more than just passive linkers. They readily associate with biological targets through hydrogen-bonding and dipole interactions. (c) Strategically placed triazolyl isosteres can also improve charge transfer interaction properties in DNA.[11,12] The idea of our design of unnatural triazolyl nucleobases linked with donor/acceptor aromatic units capable of showing possible charge transfer interaction mainly came from the fact that the charge transfer (CT) interaction plays a role to some extent in stabilizing a biomolecule or biomolecular associations.

About 60 years ago, Mulliken suggested that the CT complexes "may afford new possibilities for understanding intermolecular interactions in biological systems".[13] Since then, several biochemical phenomena have been explained on the basis of CT interactions.[14] For example, various research groups have reported ground-state charge transfer complexation mediated extra duplex stabilization and static quenching phenomena in the context of DNA probe design.[15−17] Thus, it has been shown via studying the molecular beacons and complementary linear probes that when the fluorescent dyes and quenchers come in close contact and form ground-state charge transfer complexes, they offer significant enhancement of duplex stabilization. The study of Morrison and Stols showed an enhancement of duplex stabilization when the dye and the quencher are directly adjacent to opposite strands and come in potential physical contact.[15a] Tyagi and Marras et al. have investigated that the tested configurations of various duplex DNAs with fluoro-phores and quenchers conjugated at the 5′- and 3′-termini on complementary oligodeoxynucleotides (ODNs) show an increase in duplex stability by 2−10 °C when the fluorophores and quenchers interact strongly.[15b] These results suggest that the when adjacent dye/quencher groups have the potential to form complexes, they can offer significant additional duplex stability. All such examples show ground-state complexation, the formation of which is evident from the UV−vis spectra. The designed DNA containing a donor in one strand and acceptor in the other strand has led to static quenching via ground-state charge transfer complexation and stabilization of the duplex. The "strand-displacement probe" assays utilize the same ground-state complexation phenomenon.[15c] Johansson et al. have reported that properly chosen dye/quencher pairs in dual-

Scheme 1. Synthesis of Triazolyl Donor/Acceptor Unnatural Nucleosides[a]
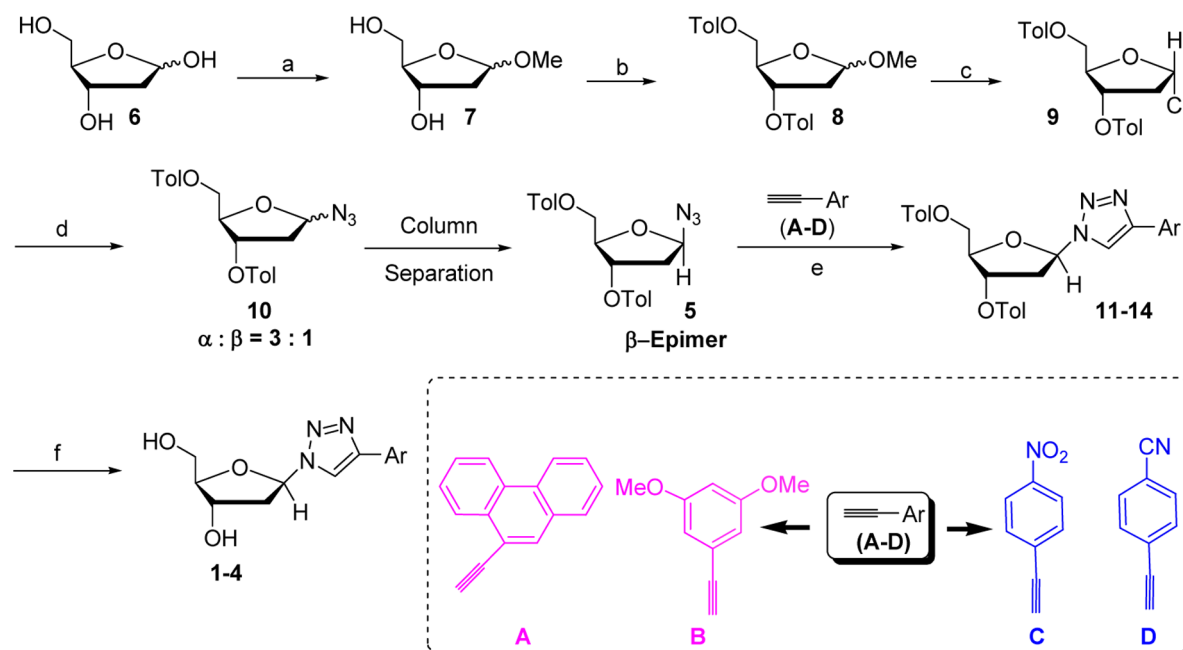
[a]Reagents and conditions: (a) dry MeOH, 1% HCl, rt; (b) dry pyridine, p-toluoyl chloride, DMAP, 0 °C, 12 h; (c) dry ether, dry HCl gas, 0 °C; (d) BF$_3$·Et$_2$O, TMS-N$_3$, CH$_2$Cl$_2$, 0 °C; (e) alkynes **A–D**, CuSO$_4$, Na-ascorbate, THF/water, DIPEA, 80 °C; (f) NaOMe/MeOH, rt.

labeled oligonucleotides can have a strong enough affinity for each other to form a ground-state complex.[16] Their experiment was supported by UV−vis spectral changes and fluorescence lifetime measurements of a series of singly labeled and dual-labeled oligonucleotides. This report suggests that the efficient static quenching can be achievable without the use of molecular beacon structures that might lead to a new design for DNA analysis. Owczarzy et al. have investigated that fluorophore/quencher-labeled probe duplexes gathered increased duplex stabilization via the formation of a ground-state charge transfer complex (evident from the change in UV−vis spectra followed by static quenching of fluorescence) between donor/acceptor pairs.[17a] Recently, they have shown that a DNA duplex could be stabilized by interaction and ground-state complexation between a dye and a quencher attached to the terminus of the two single-stranded DNAs.[17b]

Therefore, we have focused mainly on evaluating (a) the ability of triazolyl aromatics (triazole linked with donor and acceptor aromatic units) to stabilize duplex DNA via π-stacking and/or charge transfer interaction and (b) the effect of charge transfer interaction within the unnatural nucleosides or between the nucleobases in a short oligonucleotide sequence on the photophysical and/or biophysical properties. We have envisaged that the pseudoaromatic 1,2,3-triazole can modulate the electronic characteristics of the bases and endow new properties to the unnatural nucleosides and/or oligonucleotides (Figure 1). In addition, triazole as well as aromatic units may play an important role in stabilizing a duplex via π-stacking interaction. Furthermore, triazolyl nucleosides capable of self-pairing and/or heteropairing as well as stable and predictable pairing with other nucleobases may shed light on the duplex-stabilizing forces, may facilitate a biophysical approach to DNA detection, and can improve charge transfer interaction properties in DNA.[7,18] Thus, we have observed that our unnatural bases have good selectivity to form heteropairs and/or self-pairs via charge transfer and/or π-stacking interactions.

We are the first, to the best of our knowledge, to explore the possibility of unnatural heteroduplex stabilization via π-stacking and charge transfer interactions.

■ RESULTS AND DISCUSSION

Synthesis of Triazolyl Donor/Acceptor Nucleosides. With this background and aim, we have designed and synthesized a few unnatural triazolyl nucleosides via azide−alkyne cycloaddition chemistry[10] with interesting photophysical properties. Thus, starting from Hoffer's chlorosugar (obtained via a modified literature procedure),[19] we have synthesized azido nucleosides as a 3:1 mixture of α- and β-anomers. From the mixture, the β-anomer **5** was isolated in pure form by column chromatography (Figure 1 and Scheme 1).[20] The β-azide upon click reaction with several donor and/or acceptor alkynes (Do/Ac, **A−D**) followed by deprotection afforded the novel triazolyl donor and/or acceptor β-nucleosides **^{T}B$_{Do/Ac}$, 1−4**, in very good yields. Our nucleosides were characterized by NMR, IR, and mass spectrometry.

The stereochemical assignment of the epimeric 1′β-conformation was supported by a NOESY experiment as well as by the crystal structure of triazolylphenanthrene nucleoside **^{TPhen}B$_{Do}$** (Figure 2; also see the Supporting Information, section 2.1). The crystal packing shows, in addition to the nucleoside's absolute configuration, the intermolecular π-stacked and H-bonded helical layer network. Phenanthrene units are held by π−π stacking interaction among themselves and aromatic C−H⋯N bonding with triazole. The polar sugar parts are held together by strong H-bonding interaction among themselves and O−H⋯N bonding with triazole N-2 and N-3 (2.667 and 1.905 Å, respectively). The crystal network suggests that the triazolylphenanthrene nucleoside can indeed engage in H-bonding as well π-stacking interaction (Figure 2). The crystal structure of the **^{TPhen}B$_{Do}$** nucleoside showed a twist between the triazole and the phenanthrene. Therefore, all rings of the phenanthrene unit may be unable to engage fully in stacking
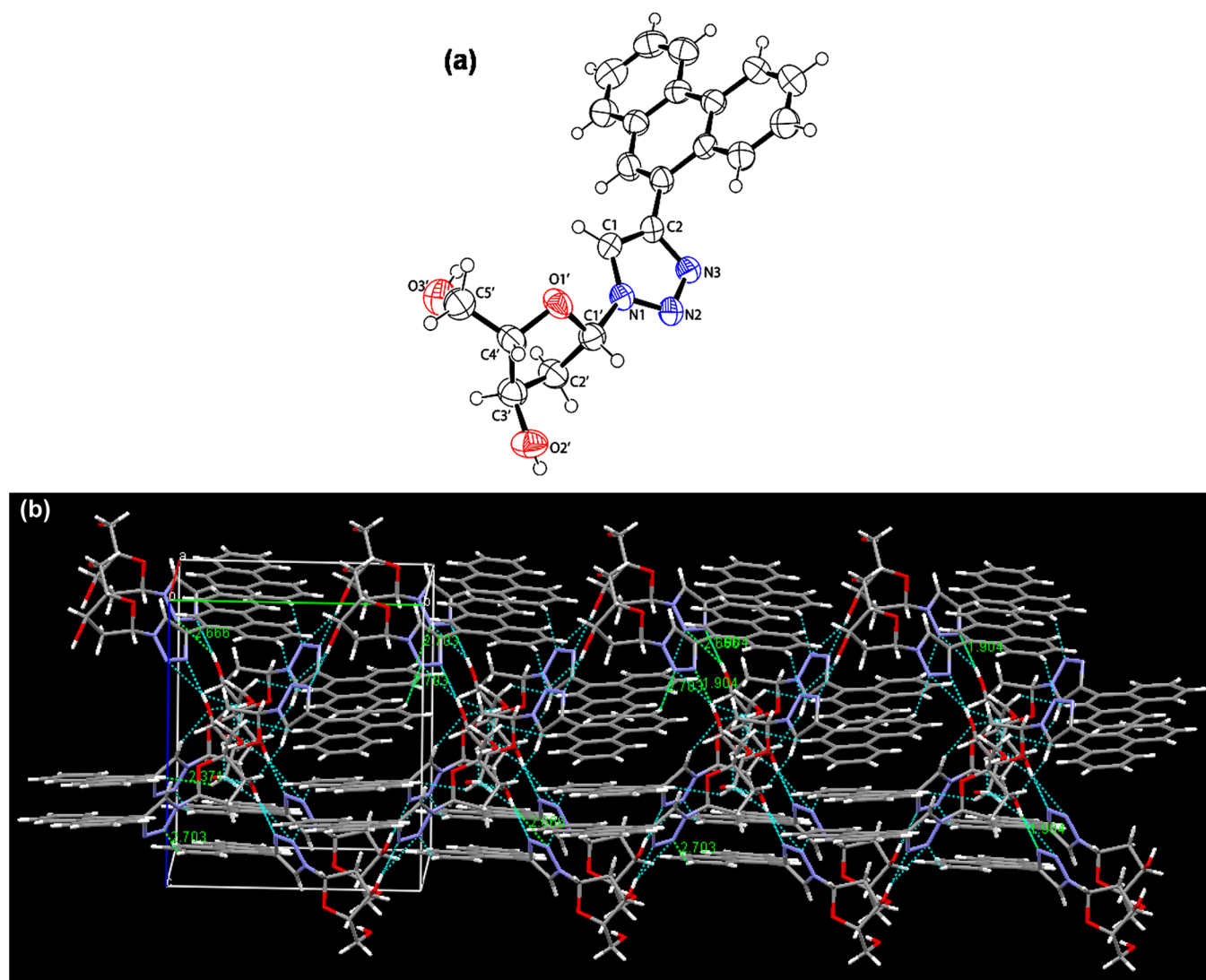
Figure 2. (a) ORTEP molecular diagram with the thermal ellipsoid at 50% probability and (b) crystal network of $^{TPhen}B_{Do}$ (**1**). Crystal structure showing the $\pi-\pi$/CH$\cdots\pi$ and Ar$-$CH$\cdots$N/OH$\cdots$N hydrogen-bonded network with a stacked layer of $^{TPhen}B_{Do}$ (**1**).

interaction upon incorporation into a DNA. However, it is possible that the third ring of phenanthrene can be involved in groove binding stabilization, leaving other rings for stacking interaction with the bases in a duplex DNA that is also evident from a MacroModel study.

Study of Stacking and/or Charge Transfer Properties. With all the nucleosides in hand, the π-stacking and/or charge transfer interaction abilities of ^{T}B nucleosides were examined prior to incorporation into oligonucleotides by studying the photophysical properties as well as utilizing a preliminary theoretical study in combination with natural bases. To evaluate the ^{T}B nucleosides' potential to form a charge transfer and/or a π-stacked pair as well as the ability to sense the microenvironment, the photophysical properties of individual as well as of Do/Ac pair nucleosides have been investigated in different solvents (see the Supporting Information, section 3). Nitrobenzene is more electron-deficient compared to cyanobenzene and hence would involve an efficient charge transfer interaction with triazolylphenanthrene when they are placed close to each other. Therefore, owing to the interest in emission and charge transfer interaction, we have chosen a phenanthrene/nitrobenzene pair that we want to disclose here. Thus, both the

triazolylphenanthrene nucleoside $^{TPhen}B_{Do}$ and the triazolylnitrobenzene nucleoside $^{TNB}B_{Ac}$ showed no sharp change in absorption maxima with increasing solvent polarity. However, the absorption spectra in aqueous buffer showed long-wavelength maxima ranging from 302 nm (for $^{TPhen}B_{Do}$) to 316 nm (for $^{TNB}B_{Ac}$), all significantly red-shifted from those of the parent native nucleosides (see the Supporting Information, Figure S12). Excitation at the long-wavelength absorption maximum gave rise to an intense emission with a maximum at around 400 nm in the case of $^{TPhen}B_{Do}$, while in the case of $^{TNB}B_{Ac}$ a very weak emission at around 450 nm (possibly due to quenching via H-bonding) was observed (see the Supporting Information, Figures S4 and S6, respectively). The UV$-$vis spectra of a 1:1 mixture of donor triazolylphenanthrene nucleoside ($^{TPhen}B_{Do}$) and acceptor triazolylnitrobenzene nucleoside ($^{TNB}B_{Ac}$) in a low-polarity dioxane solvent and in a polar phosphate buffer showed the possibility of a ground-state association property which was reflected in the appearance of a new absorption band at the longer wavelength region— longer than those of any of the parent nucleosides (see the Supporting Information, Figure S18). A quenching of fluorescence of $^{TPhen}B_{Do}$ in the presence of $^{TNB}B_{Ac}$ was also

Table 1. Oligonucleotide Sequences Containing $^{TPhen}B_{Do}/^{TNB}B_{Ac}$ Nucleosides and Their Natural Complements

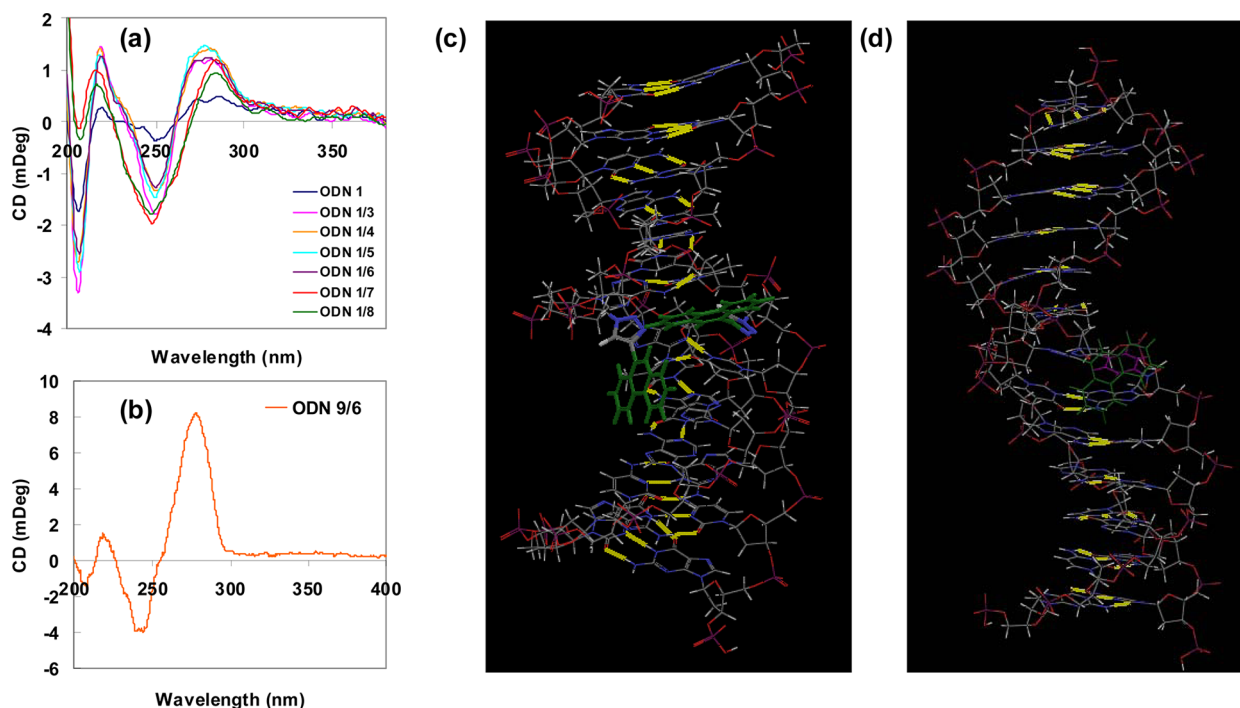|			
1	5′-CGCAAT-$^{TPhen}B_{Do}$-TAACGC-3′	7	3′-GCGTTA-$^{TPhen}B_{Do}$-ATTGCG-5′
2	5′-CGCAAT-$^{TNB}B_{Ac}$-TAACGC-3′	8	3′-GCGTTA-$^{TNB}B_{Ac}$-ATTGCG-5′
3	3′-GCGTTA**A**ATTGCG-5′	9	5′-CGCAAT**A**TAACGC-3′
4	3′-GCGTTA**G**ATTGCG-5′	10	5′-CGCAAT**G**TAACGC-3′
5	3′-GCGTTA**C**ATTGCG-5′	11	5′-CGCAAT**C**TAACGC-3′
6	3′-GCGTTA**T**ATTGCG-5′	12	5′-CGCAAT**T**TAACGC-3′

Figure 3. Circular dichroism spectra of (a) ODN **1** and its several duplexes (at 25 °C, all samples contained a 2.5 μM concentration of each strand of DNA) and (b) natural A/T duplex (the concentration was 20 μM, 50 mM sodium phosphate, 100 mM sodium chloride, pH 7.0, room temperature). (c, d) AMBER* energy-minimized conformations in water of the self-pair ($^{TPhen}B_{Do}/^{TPhen}B_{Do}$) and heteropair ($^{TPhen}B_{Do}/^{TNB}B_{Ac}$).

clear from the fluorescence emission spectra of a solution of a 1:1 mixture that indicated either the possibility of static (ground-state charge transfer complexation) or collisional quenching between the donor and the acceptor nucleosides. However, analysis of the UV−vis spectra of the mixture and the combined spectra of the individual nucleosides both in dioxane and in buffer revealed a possible formation of ground-state charge transfer complexation (see Figure S18).

Next, we carried out a theoretical calculation to get an idea about the possibility of charge transfer as well as stacking interaction between triazolylphenanthrene as a donor and triazolylnitrobenzene as an acceptor (see the Supporting Information, section 9).[21−27] Though the gas-phase calculations do not take into account solvent interactions, our preliminary observations suggested and gave us the idea that the pairing partners $^{TPhen}B_{Do}$ and $^{TNB}B_{Ac}$ in a close proximity might be involved in charge transfer as well as stacking interactions among themselves.

Synthesis and Properties of Oligonucleotides Containing Triazolyl Donor/Acceptor Nucleosides. Driven by these preliminary experimental and theoretical observations of possible stacking as well as ground-state interactions between donor ($^{TPhen}B_{Do}$) and acceptor ($^{TNB}B_{Ac}$) triazolyl nucleosides, we next turned our attention to incorporate these two nucleosides into short 13-mer oligonucleotide sequences to evaluate the stable duplex formation abilities. The rationale for

the selection of these two particular analogues for incorporation into oligonucleotide sequences was to investigate the possibility of the occurrence of charge transfer between two pairing partners in a heteroduplex and to study the role of it in duplex stabilization as well as in the fluorescence quenching phenomenon. The reason behind our choice of triazolylnitrobenzene ($^{TNB}B_{Ac}$) over triazolylcyanobenzene ($^{TCNB}B_{Ac}$) as an acceptor was the more charge deficient character of the former. Therefore, we have synthesized two complementary 13-mer oligonucleotides with $^{TPhen}B_{Do}$ (ODNs **1** and **7**) and two with $^{TNB}B_{Ac}$ (ODNs **2** and **8**) in two sequence contexts placing the ^{T}B's at a central position of the strands via an automated DNA synthesizer using phosphoramidite chemistry (Table 1). Each single-stranded ODN containing ^{T}B was hybridized to all possible natural nucleobases (ODNs **3−6** and **9−12**), and the thermal melting and photophysical properties of the so-formed duplexes were evaluated. The duplex-forming capabilities and photophysical properties of the homoduplexes formed between two identical ^{T}B's (self-pairs, ODN **1/7** and ODN **2/8**) and heteroduplexes formed between two different ^{T}B's (heteropairs, ODN **1/8** and ODN **2/7**) were also evaluated. The thermal melting stability of the perfectly matched native oligonucleotide duplexes having an A/T base pair in the same central position (ODN **3/12**) and the natural mismatched duplexes (A/A, T/T, G/G, and C/C) were also examined and compared.

We have a prior knowledge from a MacroModel study (version 9.0) (Figure 3) that the introduction of our novel unnatural [T]B self-pair/heteropair or mispair with natural bases within a duplex does not perturb the conformation of B-form DNA; rather it stabilizes the duplexes. Therefore, before measuring the thermal stability, we examined the global property of all possible duplexes using circular dichroism spectroscopy. We found that all spectra showed a positive band at around λ = 278−286 nm and a negative band at around λ = 248−252 nm of nearly equal magnitude with an intersection at around λ = 260−262 nm similar to that of the natural A/T pair duplex (Figure 3).

Study of the Thermal Stability of Various Unnatural Duplexes. Encouraged by all the above results, we next evaluated the thermal stabilities of the unnatural self-pairs, heteropairs, and mispairs [(5'-CGCAATXTAACGC-3')/(5'-GCGTTAYATTGCG-3')] by a thermal denaturation experiment. This sequence context was chosen to examine the effects of flanking pyrimidines (T base for **X**) and purines (A base for **Y**) (Table 2) on the duplex stabilities. To compare the

Table 2. T_m Values and Thermodynamic Parameters for Several Duplexes

5'-CGC AAT **X** TAA CGC-3'

3'-GCG TTA **Y** ATT GCG-5'

ODN	X/Y	T_m	ODN	X/Y	T_m
1/7	[TPhen]B[Do]/[TPhen]B[Do]	53.6	**2/8**	[TNB]B[Ac]/[TNB]B[Ac]	50.2
1/8	[TPhen]B[Do]/[TNB]B[Ac]	52.3	**2/7**	[TNB]B[Ac]/[TPhen]B[Do]	54.4
1/3	[TPhen]B[Do]/A	48.5	**2/3**	[TNB]B[Ac]/A	44.8
1/4	[TPhen]B[Do]/G	49.4	**2/4**	[TNB]B[Ac]/G	47.0
1/5	[TPhen]B[Do]/C	51.3	**2/5**	[TNB]B[Ac]/C	44.7
1/6	[TPhen]B[Do]/T	50.0	**2/6**	[TNB]B[Ac]/T	43.4
9/7	A/[TPhen]B[Do]	47.1	**9/8**	A/[TNB]B[Ac]	43.9
10/7	G/[TPhen]B[Do]	48.0	**10/8**	G/[TNB]B[Ac]	44.3
11/7	C/[TPhen]B[Do]	48.3	**11/8**	C/[TNB]B[Ac]	43.5
12/7	T/[TPhen]B[Do]	46.9	**12/8**	T/[TNB]B[Ac]	43.4
9/6	A/T	51.2	**12/3**	T/A	53.2

^{a}All samples contained a 2.5 μM concentration of each strand of DNA, 50 mM sodium phosphate, 100 mM sodium chloride, pH 7.0, with 0.1 mM EDTA, room temperature. The error in T_m is estimated as ± 0.3 °C. The T_m values of various natural mismatched duplexes are 40.8 (T/T), 42.9 (A/A), 44.5 (G/G), and 35.5 (C/C).

stabilities, the thermal melting temperatures (T_m) of the A/T natural matched and all natural mismatched pairs have also been evaluated. Thus, we observed the following decreasing order of stability for ODN **1** with its various target partners: [TPhen]B[Do]/[TPhen]B[Do] > [TPhen]B[Do]/[TNB]B[Ac] > A/T > [TPhen]B[Do]/C ≥ [TPhen]B[Do]/T > [TPhen]B[Do]/G ≥ [TPhen]B[Do]/A. Similarly, for ODN **2**, the stability follows the trend [TNB]B[Ac]/[TPhen]B[Do] > A/T ≥ [TNB]B[Ac]/[TNB]B[Ac] > [TNB]B[Ac]/G ≥ [TNB]B[Ac]/C > [TNB]B[Ac]/A ≥ [TNB]B[Ac]/T. Our results interestingly demonstrate that the stabilities of the self-pair (**1/7**) and heteropair (**2/7**) of [TPhen]B[Do] are slightly higher than those of any of the natural A/T or T/A pairs. The highest stability of the [TPhen]B[Do]/[TPhen]B[Do] self-pair is most probably the result of strong hydrophobic and π−π stacking interaction between two triazolylphenanthrene units of two strands of the self-pair. Also, the heteropair **1/8** is slightly more stable than the natural A/T pair. The stability of the highest stable unnatural heteropair [TNB]B[Ac]/[TPhen]B[Do] is

found to be 3.2−1.2 °C higher than that of a natural A/T or T/A pair and comparable (only slightly less stable by 1.1−1.6 °C) to that of a natural C/G or G/C pair. The [TPhen]B[Do]/[TPhen]B[Do] self-pair is also slightly less stable (less by only 1.9−2.4 °C) than a natural C/G or G/C pair but more stable (by 2.4−0.4 °C) than a natural A/T or T/A pair (Table 2; see also the Supporting Information, Table S4). Therefore, we can conclude that the triazolyl donor/acceptor nucleosides containing unnatural DNAs are promising to offer stabilities at least comparable to that of a natural A/T or T/A pair.

Other than the duplex-stabilizing property, an unnatural base pair should be highly selective against mispairing with the natural nucleobases so that the DNA with that unnatural pair would be efficient at acting like natural DNA.[28] Thus, we next studied the selectivity of the unnatural bases in mispairing with the natural nucleobases. To examine the sequence dependency in mispairing, ODNs **7** and **8** were hybridized with the corresponding complementary natural sequences (ODNs **9−12**). The thermal denaturation experiment shows the following trends of stability for ODN **7** (C ≥ G > A > T) and ODN **8** (G > A ≥ C ≥ T), reflecting the possible role of hydrophobic/dipole−dipole interactions (Table 2). In general, however, higher T_m values are observed when the flanking bases are pyrimidine (dT). Better interstrand base stacking (T−[T]B−T) interaction results in more stable duplexes compared to the corresponding A−[T]B−A duplexes in the case of mispairing with natural bases (Table 2). However, for heteropair formation the opposite is true; i.e., in the case of [TPhen]B[Do], strong aromatic intrastrand stacking with purine (dA) as well as hydrophobic and charge transfer interaction between [TPhen]B[Do] and [TNB]B[Ac] endows the [TNB]B[Ac]/[TPhen]B[Do] heteropair with the highest duplex stabilization. These observations are significant considering the intrastrand stacking interaction within the nearby natural bases in the duplex, suggesting that the nucleobases possibly slip to stack on each other within the self-pair and/or heteropair.[1h,29] It is noteworthy to mention that a significant portion of base stacking most probably results from a partial overlap of the polar moiety of the nitrobenzene unit of the [TNB]B[Ac] nucleoside with the polarizable triazolylphenanthrene ring system and adjacent natural bases.[29d]

To better understand the thermodynamic origin of higher stability of the heteropair, and self-pair, we have calculated thermodynamic parameters from van't Hoff analyses of the thermal denaturation curves for fluorescent duplexes containing [TPhen]B[Do]. Thus, it is evident that the self-pair stabilization ([TPhen]B[Do]/[TPhen]B[Do] and [TNB]B[Ac]/[TNB]B[Ac]) is driven by a more favorable (less negative) entropic change compared to that of the natural A/T pair. While the process of coil to helix formation is accompanied by a comparable change in free energy for the [TPhen]B[Do]/[TPhen]B[Do] self-pair, due to an unfavorable enthalpy change, the free energy change of the process is very low in the case of the [TNB]B[Ac]/[TNB]B[Ac] self-pair (see the Supporting Information, section 5). This is probably because of the smaller surface area and extremely unfavorable electrostatic repulsive forces between two highly polar triazolylnitrobenzene groups (μ = 8.3 D).

The higher stability of the [TNB]B[Ac]/[TPhen]B[Do] heteropair compared to the [TPhen]B[Do]/[TNB]B[Ac] pair is due to the large surface area of triazolylphenanthrene (**TPhen**) compared to triazolylnitrobenzene (**TNB**) wherein more intrastrand stacking with a flanking purine (A) in the sequence −A−[TPhen]B[Do]−A− is operating. Furthermore, all the unnatural self-pairs or heteropairs are entropically more favorable compared to any
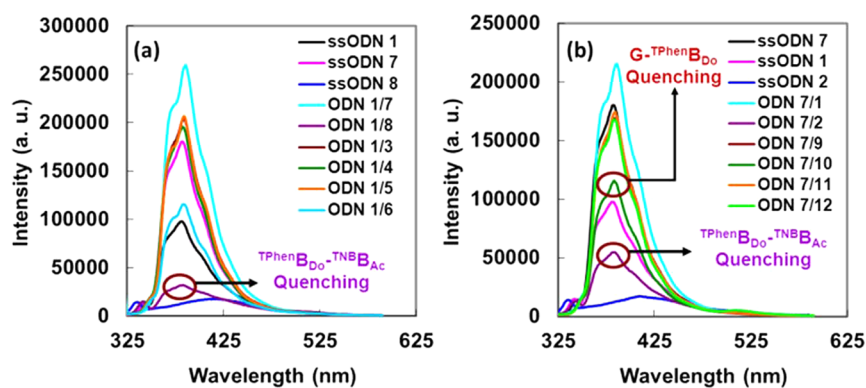
Figure 4. Fluorescence emission spectra (λ_{ex} = 315 nm) of (a) ODN **1** and (b) ODN **7** in their single-stranded and duplex states with various complementary ODNs (2.5 μM concentration of different ODNs in 50 mM sodium phosphate, 100 mM sodium chloride, pH 7.0, room temperature).
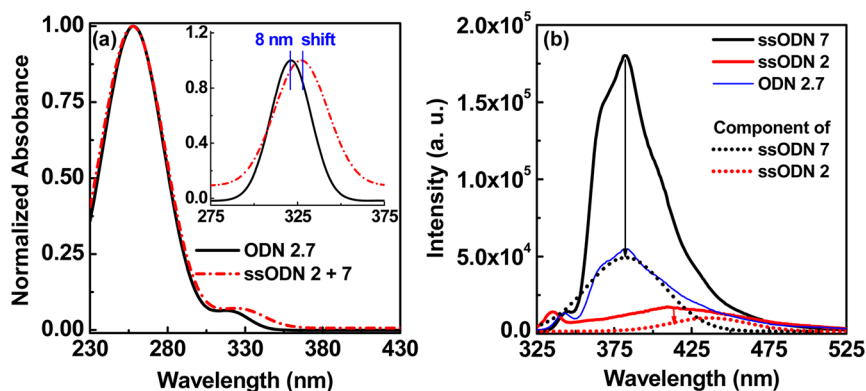

Figure 5. (a) UV−vis absorption spectra normalized at 260 nm of the hybrid ODN **7**/**2** (solid line) and the absorption spectra obtained by combining the absorption spectra of the individual oligonucleotides ODN **7** and ODN **2** (dotted line). Inset: Guassian fit spectra of the chromophoric region to show the differences. (b) Emission spectra of the single-stranded ODN **7** and ODN **2** containing donor- and/or acceptor-nucleoside ($^{TPhen}B_{Do}$ and/or $^{TNB}B_{Ac}$)-labeled oligodeoxyribonucleotides and emission spectra of the hybrid they form, ODN **7**/**2**. The duplex ODN **7**/**2** was excited at 310 nm, which is the optimal excitation wavelength for the donor nucleoside, $^{TPhen}B_{Do}$. The emission from OND **7** and ODN **2** arises when stimulated by 310 and 330 nm light, which are the optimal excitations for the donor nucleoside ($^{TPhen}B_{Do}$) and acceptor nucleoside ($^{TNB}B_{Ac}$), respectively. Resolving the emission spectrum of the duplex ODN **7**/**2** into its components showed a decrease in intensity of both the donor and acceptor nucleosides upon hybridization. ([ODN **7**] = 15 μM; 50 mM sodium phosphate, 100 mM NaCl, pH 7.0; λ_{ex} = 310 nm, λ_{em} = 384 nm).

natural pairs. In the heteropairs $^{TNB}B_{Ac}$ is involved in ground-state charge transfer interactions as well as intercalative interstrand stacking interactions.[1h,29] Interestingly, all the mispairs of either $^{TPhen}B_{Do}$ or $^{TNB}B_{Ac}$ in any sequence context were found to be thermodynamically more stable compared to any combinations of natural mismatched pairs (A/A, T/T, G/G, and C/C). Overall, the unnatural bases are more selective for heteropairing as well as self-pairing possibly via π-stacking and/or charge transfer interaction between two donor and/or acceptor pairing partners and natural bases within a duplex.

The stability order of the self-pairs or heteropairs observed from a thermal melting and thermodynamics study can be explained by considering the stacking as well as electrostatic repulsion and charge transfer interaction, which was also supported by the AMBER*-optimized geometry of the corresponding duplexes (Figure 3c,d; also see the Supporting Information, Figure S25). Thus, in the highest stable heteropair $^{TNB}B_{Ac}$/$^{TPhen}B_{Do}$ both the triazoles are involved in intrastrand stacking, the third ring of the phenanthrene unit is engaged in major groove binding, and nitrobenzene is involved in intercalative stacking between phenanthrene and its other natural flanking base pair. The nitrobenzene unit is also

involved in charge transfer interaction with the phenanthrene unit via a stacking between the polar −NO$_2$ and polarizable phenanthrene unit. The other two rings of the phenanthrene stack with the natural A base in the same strand (A−$^{TPhen}B_{Do}$−A) very strongly as the stacking propensity of A is the highest among those of all four natural bases (A > G > C = T). It is observed that the vertical distance between triazole and the natural base of the same strand (3.2−3.8 Å) is comparable to that between the natural bases (3.4 Å), and thus, it is sufficient for strong intrastrand stacking. The two dipolar units, phenanthrene and nitrobenzene, with dipole moments of 3.5 and 8.3 D (derived from Gaussian 03-optimized geometries), respectively, face each other, which probably allows them to participate in strong charge transfer interaction (Figure 3d). Thus, a charge transfer interaction between $^{TPhen}B_{Do}$ and $^{TNB}B_{Ac}$ as well as a stacking interaction is operative, leading to the highest duplex stability among those of all the unnatural and natural A/T or T/A duplexes. A strong charge transfer interaction is also evident from the quenching of fluorescence (Φ_f = 0.04) of $^{TPhen}B_{Do}$ in the heteroduplex (Figure 4).

Charge Transfer and π−π-Stacking Interaction and Duplex Stabilization. The proof of our concept of charge
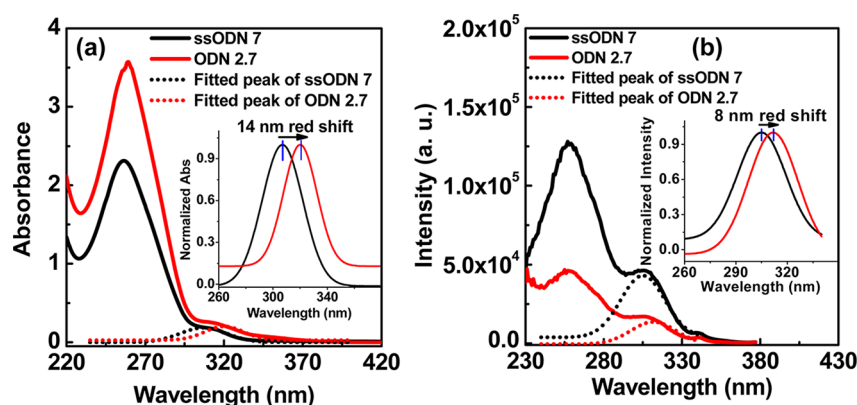
Figure 6. Ground-state complexation is evident from a bathochromic shift of the absorption and fluorescence excitation spectra of the probe ODN **7** upon duplex formation: (a) UV−vis and (b) fluorescence excitation spectra of ODN **7** and hybrid ODN **7/2** at room temperature. Dotted lines are the Gaussian fit spectra of the chromophoric region to show the differences. Inset: magnified Gaussian fit spectra of the chromophoric region which clearly show the red shifting of λ_{abs}^{max} (~14 nm) and λ_{ex}^{max} (~8 nm) of ODN **7** upon hybridization with ODN **2** ([ODN **7**] = [ODN **2**] = 15 μM; 50 mM sodium phosphate, 100 mM NaCl, pH 7.0; λ_{em} = 384 nm).

transfer complexation came from the analysis of UV−vis spectra and a fluorescence quenching experiment. Thus, from a careful analysis of the UV−vis spectra of single-stranded ODNs, their addition spectra, and the spectra of the duplex ODN **7/2** [ODN **7** contains donor triazolylphenanthrene nucleoside (^{TPhen}B$_{Do}$), and ODN **2** contains acceptor triazolylnitrobenzene nucleoside (^{TNB}B$_{Ac}$)], we observe an about 8 nm shift in absorption wavelength when the combined absorption spectra of the individual ODNs (ODN **7** and **2**) are compared to the spectra of hybrid duplex ODN **7/2**. This observation of a change in UV−vis spectra indicates a possible formation of a ground-state charge transfer complex between the two nucleosides ^{TPhen}B$_{Do}$ and ^{TNB}B$_{Ac}$ in the duplex ODN **7/2** (Figure 5a).[14a,15−17] The ground-state complexation phenomenon is further supported by a static quenching of the fluorescence of the donor nucleoside by the acceptor nucleoside in a hybrid duplex ODN **7/2**. The static quenching of fluorescence is also supported by the quenching of the emission of both the donor and acceptor nucleosides upon hybridization that is clear from the resolved emission spectra of the duplex ODN **7/2** (Figure 5b).[14a,15b] A similar phenomenon was also reported by Tyagi et al.[15b]

In addition to this, ground-state complexation becomes obvious by a bathochromic shift of the absorption and fluorescence excitation spectra of the probe ODN **7** containing the donor fluorescent nucleoside in the presence of target ODN **2** containing the acceptor (quencher) fluorescent nucleoside with a static quenching efficiency. The prominent bathochromic shift is observed in the duplex ODN **7/2** compared to the single-stranded ODN **7** (Figure 6).[14a,16]

We have also tested the static quenching event considering donor-nucleoside-labeled ODN **7** as a probe (fluorophore) and the acceptor-nucleoside-labeled ODN **2** as a target quencher. Thus, from the steady-state fluorescence experiment we observed a smaller F_0/F value at high temperature compared to that at room temperature for the duplex OND **7/2**. Moreover, the time-resolved fluorescence experiment revealed the constant value of τ_0/τ (τ_0/τ = 1) for both the single-stranded ODN **7** and the duplex ODN **7/2** (see the Supporting Information, Figure S20). This result clearly indicates that the quenching incidence is purely a static quenching in nature, which is also supported by reported similar observations.[14a,16] Recently, Owczarzy et al. have shown that a DNA duplex can

be stabilized by interaction and complexation between a dye and a quencher attached to the terminus of the two single-stranded DNAs. They also have investigated that fluorophore/quencher-labeled probe duplexes gathered increased duplex stabilization via the formation of ground-state charge transfer complex formation (evident from the change in UV−vis spectra followed by static quenching of fluorescence) between donor/acceptor pairs.[16] Our experimental results follow a similar trend. A correlation between the reported literature data and our experimental observations supports the ground-state charge transfer complex formation between the donor and the acceptor triazolyl unnatural nucleosides in the duplex ODN **7/2** and the static quenching of fluorescence event.[14a,15−17] Hybridization of ODN **7** and ODN **2** brings the donor/acceptor pair in close contact, leading to a charge transfer complexation. Therefore, ground-state charge transfer complexation possibly played an important role in giving the highest duplex stabilization in the heteroduplex ODN **7/2** among all other unnatural/natural duplexes tested. All the reported works on the ground-state complexation, duplex stabilization, and static quenching phenomenon considered the labeling of two DNA strands at the termini,[15−17] and few reports[16,17] clearly state that the dye/quencher pair destabilizes the duplex when placed at the middle of the strand. There is no report of such ground-state complexation in unnatural donor/acceptor nucleosides. Thus, our probes might find importance toward the design of new donor/acceptor nucleosides with duplex-stabilizing ability through π-stacking and ground-state charge transfer complexation. We are currently focusing our interest on the design and synthesis of more such suitable heteropairs.

While both the self-pairs are accommodated within duplex DNA without significant loss of duplex stability, one of the two large aromatic triazolylphenanthrenes of the homoduplex ^{TPhen}B$_{Do}$/^{TPhen}B$_{Do}$ pair is involved in intercalative stacking and the other is involved in stacking inside the groove position. The stacking interaction within the ^{TPhen}B$_{Do}$ self-pair is consistent with its high stability and is supported by the AMBER*-optimized geometry of the duplex. Thus, it is clear from the MacroModel study that one phenanthrene is engaged in major groove binding while the other one is involved in intercalative inter/intrastrand stacking between its flanking base pair, leading to the second most stable complex compared to all the unnatural and natural A/T or T/A duplexes. These

H

dx.doi.org/10.1021/jo302033f | J. Org. Chem. XXXX, XXX, XXX−XXX

nucleotides do not pair in an edge-on manner as observed with natural Watson−Crick base pairs (Figure 3c).

In contrast to the $^{TPhen}B_{Do}$ self-pair, the nucleobase analogues of the $^{TNB}B_{Ac}$ self-pair are not sufficiently large to bridge the duplex and cannot intercalate. They are not optimally edge-to-edge packed; rather their packing probably arises from the triazole parts which might engage in intrastrand stacking/electrostatic interactions between their flanking natural base pair. It is clear from the AMBER*-optimized geometry that both the highly polar nitrobenzene units are tilted out of the helix and their negative dipoles face each other. The distance between two repelling −NO$_2$ groups was found to be 3.6 Å; therefore, the two dipoles (dipole moment 8.3 D) are extended enough to repel each other. Thus, a dipole−dipole/electrostatic repulsion is operative to some extent, leading to duplex destabilization compared to all unnatural self-pair/heteropair as well as natural A/T or T/A duplexes.

Our concept of duplex stabilization through possible involvement of π-stacking and/or charge transfer interactions was supported by the highest stabilization of the heteropair ODN **2/7** as well as a static quenching of fluorescence of $^{TPhen}B_{Do}$ in this heteropair (Figure 4b). The charge transfer interaction is evident from the UV−vis and fluorescence excitation spectra (Figures 5a and 6). That the quenching of fluorescence in the heteropair ODN **2/7** is purely a static quenching is also evident from the UV−vis as well as fluorescence spectral data (Figures 5 and 6; also see the Supporting Information, Figures S19−S22). The possible charge transfer mediated quenching is also evident in the case of heteropair ODN **1/8** (Figure 4). That the electrostatic/dipole−dipole interaction possibly plays a role in duplex stability and/or instability is evident from the lower T_m of the self-pair of $^{TBN}B_{Ac}$ than that of the heteropair, which is mostly due to electrostatic repulsion between two −NO$_2$ groups. A bathochromic shift of the absorbance maxima and hypochromicity of $^{TPhen}B_{Do}$ in a single-stranded ODN of the reverse sequence (−A−$^{TPhen}B_{Do}$−A−) compared to its normal sequence (−T−$^{TPhen}B_{Do}$−T−) indicates the possibility of stacking interaction between $^{TPhen}B_{Do}$ and natural base A, which also is reflected in the more intense fluorescence of single-stranded ODN **7** (Figure 4b). The possible stacking interaction is also evident from the chromophore's absorbances in single-stranded and duplex DNA (see the Supporting Information, Figure S17).

To explore the applicability of our triazolyl unnatural oligonucleotide, we next studied the ability of triazolylphenanthrene to stabilize an abasic-site-containing DNA duplex, one of the most frequent DNA lesions responsible for deleterious mutations leading to genomic disintegrity,[30] by a thermal denaturation experiment. An abasic site is a discontinuity of the DNA base stack in the missing base position, leading to a deviation from the regular DNA duplex structure. Various model studies reveal that the aromatic building blocks can serve as substituents for the missing base of the abasic site and can stabilize the abasic DNA duplex by intercalative stacking interaction in the cavity in the missing base position. Therefore, due to their biological importance, there is a growing interest in stabilizing abasic sites in DNA for both diagnostic and pharmaceutical purposes.[31] Our preliminary observation revealed that the unnatural probe ODN **1** containing triazolylphenanthrene nucleoside formed a stable duplex with its target DNA containing an abasic site [Ap; ODN **13** (5′-GCGTTA-**Ap**-ATTGCG-3′)] opposite the $^{TPhen}B_{Do}$ nucleoside

of the probe (ODN **1/13**; T_m = 52.2 °C). The melting temperature (T_m) data of the corresponding duplexes showed that our probe ODN **1** containing the unnatural nucleoside led to a significant increase of the melting temperature in comparison to any duplex containing any of the natural nucleotides opposite the abasic site (see the Supporting Information, Table S5). Moreover, the thermal stabilization offered by the $^{TPhen}B_{Do}$ unnatural nucleoside is comparable to the stabilization of a natural A/T pair duplex. The triazolylphenanthrene is possibly positioned between the base pairs adjacent to the abasic site and thereby allows for the continuation of stacking interactions in the absence of the nucleobase, leading to such high duplex stabilization. A detailed thermodynamic investigation on the abasic site stabilization is necessary, and that is our current research focus.

■ CONCLUSION

In conclusion, we have shown that our new and novel triazolyl unnatural donor/acceptor nucleobases offer a good stabilization of the heteropair/self-pair duplexes that are comparable to that of a natural A/T pair. The stabilization of the duplexes was explained on the basis of possible involvement of π-stacking and/or charge transfer interactions. The evidence of ground-state charge transfer complexation came from the UV−vis spectra and the static quenching of fluorescence. The probe ODN **1** was found to offer a very high thermal stabilization of a DNA duplex containing an abasic site. The static quenching of fluorescence of $^{TPhen}B_{Do}$ by $^{TNB}B_{Ac}$ in any sequence context clearly shows that our unnatural DNA might find applications in charge transfer processes, which is our recent research focus. Our results might shed light on the design of new donor/acceptor unnatural nucleosides with duplex-stabilizing ability through π-stacking and ground-state charge transfer complexation. We are currently focusing our interest on the design and synthesis of more of such suitable heteropairs.

■ EXPERIMENTAL SECTION

General Experimental Procedures. ^{1}H NMR spectra were measured with a 400 MHz machine; ^{13}C NMR spectra were measured with a 100 MHz spectrometer. Coupling constants (J) are reported in hertz. The chemical shifts are shown in parts per million downfield from tetramethylsilane using residual chloroform (δ = 7.24 in ^{1}H NMR, δ = 77.23 in ^{13}C NMR), dimethyl sulfoxide (δ = 2.48 in ^{1}H NMR, δ = 39.5 in ^{13}C NMR), and methanol (δ = 3.30 in ^{1}H NMR, δ = 49.0 in ^{13}C NMR) as internal standards. FAB masses were recorded on a mass spectrometer.

The reagents for DNA synthesis were purchased and used. Mass spectra of oligodeoxynucleotides were determined with a MALDI-TOF MS instrument (acceleration voltage 20 kV, positive mode) with 2′,3′,4′-trihydroxyacetophenone as a matrix. Concentration was measured from the molar extinction coefficient at 260 nm at 80 °C for all ODNs. All aqueous solutions utilized purified water. Reversed-phase HPLC was performed on reversed-phase columns (10 × 150 mm, 4.6 × 150 mm) with a chromatograph using a UV detector at 254 nm.

Synthesis of 1-O-Methyl-2-deoxy-D-ribofuranose (7). 2-Deoxyribose sugar **6** taken in a round-bottom flask was dissolved in methanol, and 1% HCl solution was added. The solution was stirred for 2 h at room temperature under a N$_2$ atmosphere. The reaction mixture was neutralized after 2 h by addition of NaHCO$_3$ and again stirred for 40 min. The reaction mixture was filtered through Whatman 41 filter paper, and the filtrate was evaporated to dryness in vacuum to yield **7** as a honeylike product with 100% yield, and this material was used for the next step without further purification.

Synthesis of 1-O-Methyl-2-deoxy-3,5-bis[O-(p-toluoyl)]-D-ribofuranose (8). 7 (4.41 g, 0.0297 mol) was dissolved in dry pyridine, and 0.488 g (3.99 mmol) of DMAP was added. The solution was stirred for 5 min and then cooled to 0 °C. *p*-Toluoyl chloride (8.5 mL, 60.784 mmol) was added dropwise, and the solution was stirred for 12 h at 0 °C. The reaction mixture was then extracted with DCM, washed with NaHCO$_3$, and coevaporated with toluene three times to remove the pyridine. The product **8** was separated by column chromatography (silica gel 60−120, hexane:EtOAc = 10:1), and the overall yield was 7.5 g (70%, 0.02 mol). This material was fully used for the next step.

Synthesis of 2-Deoxy-3,5-bis[O-(p-toluoyl)]-α-D-ribofuranosyl Chloride (9). Dry HCl gas was passed through an ethereal solution of **8** (7.5 g, 0.02 mol) at 0 °C. The white solid product obtained was filtered and washed with dry ether. The product **9** was then dried in vacuum, and the overall yield was 4.48 g (59%, 0.01 mol): ^{1}H NMR (CDCl$_3$, 400 MHz) δ 2.41 (3H, s), 2.42 (3H, s), 2.75 (1H, d, *J* = 14.8 Hz), 2.84−2.91 (1H, m), 4.6 (1H, dd, *J* = 4.4, 12.4 Hz), 4.68 (1H, dd, *J* = 3.2, 12.0 Hz), 4.86 (1H, q, *J* = 3.2 Hz), 5.56 (1H, dd, *J* = 2.8, 6.4 Hz), 6.48 (1H, d, *J* = 5.2 Hz), 7.21−7.28 (4H, m), 7.9 (2H, d, *J* = 8.0 Hz), 7.99 (2H, d, *J* = 8.0 Hz); ^{13}C NMR (CDCl$_3$, 100 MHz) δ 21.9, 44.7, 63.7, 64.5, 73.8, 84.2, 84.9, 95.5, 126.9, 129.4, 129.9, 130.1, 144.3, 144.5, 166.3, 166.6.

Synthesis of 2-Deoxy-3,5-bis[O-(p-toluoyl)]-β-D-ribofuranosyl Azide (5).[20] To a solution of toluoyl-protected **9** (1.185 g, 3.048 mmol) in dry DCM were added BF$_3$·Et$_2$O (0.0376 mL, 0.305 mmol) and trimethylsilyl azide [(TMS)N$_3$] (0.481 mL, 3.66 mmol) at 0 °C. The solution was stirred vigorously for 6 h. The reaction mixture was partitioned between water and DCM. The organic layer was washed with water followed by brine solution, dried over Na$_2$SO$_4$, and then concentrated. The azide obtained was found to be 784.6 mg (64.9%, 1.98 mmol). The mixture of α- and β-isomers produced in a 3:1 ratio (**10**) was then separated by column chromatography using 230−400 mesh size silica gel (solvent system hexane:EtOAc = 20:1) to isolate β-epimer **5** in 21% yield (249.7 mg, 0.63 mmol), which was then characterized: IR (KBr) 2110, 1715 cm^{-1}; ^{1}H NMR (CDCl$_3$, 400 MHz) δ 2.41 (3H, s), 2.42 (3H, s), 4.52−4.61 (5H, m), 5.57−5.59 (1H, m), 5.72 (1H, t, *J* = 4.8 Hz), 7.22−7.26 (4H, m), 7.9 (2H, d, *J* = 8.4 Hz), 7.98 (2H, d, *J* = 8.4 Hz); ^{13}C NMR (CDCl$_3$, 100 MHz) δ 21.7, 38.9, 64.1, 74.7, 83.7, 92.1, 126.8, 126.9, 129.3, 129.7, 129.9, 144.0, 144.3, 166.2, 166.3; ESI-TOF-MS *m/z* 418 [M + Na]$^+$.

General Procedure for the Preparation of Triazolyl Donor/Acceptor Nucleosides 11−14 via Azide−Alkyne Cycloaddition Reaction. In a round-bottom flask fitted with a septum, **5** (1.0 equiv) was dissolved in dry THF and degassed for 10 min with N$_2$. Then the aromatic alkyne **A−D** (1.5 equiv) was added, and both stirring and degassing were continued for the next 5 min. After that, 6 mol % sodium ascorbate dissolved in a small quantity of water was added, and the solution was degassed for another 5 min. Then 1 mol % copper sulfate dissolved in a small quantity of water was added followed by degassing. The final ratio of THF to H$_2$O in the reaction mixture was maintained as 3:1. Finally, diisopropylethylamine (DIPEA) was added to the reaction mixture (1.5 equiv). The solution was refluxed at 75−80 °C overnight with stirring. After full consumption of the starting azide, the reaction mixture was evaporated and partitioned between water and ethyl acetate. The organic layer was washed with water followed by brine solution, dried over Na$_2$SO$_4$, and then concentrated. The products **11−14** were then separated by column chromatography (silicagel 60−120, hexane:EtOAc = 2:1) and characterized. The average yields were between 90% and 99%.

1-[2′-Deoxy-3′,5′-bis{O-(p-toluoyl)}-β-D-ribofuranosyl]-4-(phenanthren-9-yl)-1H-1,2,3-triazole (11). Using the general procedure, starting from 200 mg (0.506 mmol) of **5** and 122.77 mg (0.607 mmol) of 9-ethynylphenantherene (**A**), 288.7 mg (0.484 mmol) of compound **11** was isolated as a yellow solid: yield 95.6%; mp 148−151 °C; IR (KBr) 1714, 1610, 1281, 1123, 1020 cm^{-1}; ^{1}H NMR (CDCl$_3$, 400 MHz) δ 2.22 (3H, s), 2.45 (3H, s), 2.98−3.01 (1H, m), 3.29−3.33 (1H, m), 4.62−4.65 (1H, m), 4.73 (2H, s), 5.83−5.84 (1H, m), 6.66 (1H, t, *J* = 8.0 Hz), 7.06 (2H, d, *J* = 7.6 Hz), 7.29 (2H, d, *J* = 7.6 Hz), 7.57−7.61 (2H, m), 7.69 (2H, t, *J* = 6.8, 7.2 Hz), 7.84 (4H, d, *J* = 6.8 Hz), 7.98 (2H, d, *J* = 7.6 Hz), 8.08 (1H, s), 8.33 (1H, d, *J* = 8.4 Hz),

8.71 (1H, d, *J* = 8.4 Hz), 8.77 (1H, d, *J* = 8.0 Hz); ^{13}C NMR (CDCl$_3$, 100 MHz) δ 21.5, 21.7, 29.7, 38.5, 63.9, 74.8, 83.7, 89.1, 121.7, 122.6, 122.9, 126.3, 126.5, 126.6, 126.8, 126.9, 127.0, 127.2, 128.5, 128.9, 129.3, 129.4, 129.6, 129.9, 130.0, 130.5, 130.7, 131.2, 144.1, 144.5, 147.3, 165.9, 166.3; ESI-TOF-MS *m/z* 598 [M + H]$^+$; HRMS *m/z* calcd for C$_{37}$H$_{32}$N$_3$O$_5$ ([M + H]$^+$) 598.2342, found 598.2322.

1-[2′-Deoxy-3′,5′-bis{O-(p-toluoyl)}-β-D-ribofuranosyl]-4-(3,5-dimethoxyphenyl)-1H-1,2,3-triazole (12). Using the general procedure, starting from 200 mg (0.506 mmol) of **5** and 98.45 mg (0.607 mmol) of 1-ethynyl-3,5-dimethoxybenzene (**B**), 280.0 mg (0.502 mmol) of compound **12** was isolated as a white solid: yield 99%; mp155−158 °C; IR (KBr) 1715, 1611, 1276, 1204, 1156 cm^{-1}; ^{1}H NMR (CDCl$_3$, 400 MHz) δ 2.35 (3H, s), 2.44 (3H, s), 2.88−2.93 (1H, m), 3.12−3.17 (1H, m), 3.49 (1H, s), 3.82 (6H, s), 4.57−4.61 (1H, m), 4.69−4.72 (2H, m), 5.78−5.79 (1H, m), 6.44 (1H, s), 6.54−6.57 (1H, t, *J* = 6.4 Hz), 6.88 (1H, s), 7.19 (2H, d, *J* = 8.0 Hz), 7.28 (2H, d, *J* = 8.0 Hz), 7.87 (2H, d, *J* = 8.0 Hz), 7.96 (2H, d, *J* = 7.6 Hz), 7.97 (1H, s); ^{13}C NMR (CDCl$_3$, 100 MHz) δ 21.9, 38.9, 55.7, 64.1, 75.0, 83.9, 89.3, 101.0, 103.9, 118.5, 126.6, 126.8, 129.6, 129.8, 130.0, 144.5, 144.8, 148.3, 161.3, 166.1, 166.1; ESI-TOF-MS *m/z* 580 [M + Na]$^+$; HRMS *m/z* calcd for C$_{31}$H$_{32}$N$_3$O$_7$ ([M + H]$^+$) 558.2240, found 558.2233.

1-[2′-Deoxy-3′,5′-bis{O-(p-toluoyl)}-β-D-ribofuranosyl]-4-(4-nitrophenyl)-1H-1,2,3-triazole (13). Using the general procedure, starting from 200 mg (0.506 mmol) of **5** and 89.31 mg (0.607 mmol) of 1-ethynyl-4-nitrobenzene (**C**), 255.6 mg (0.472 mmol) of compound **13** was isolated as a yellow solid: yield 93.23%; mp 185−190 °C; IR (KBr) 1715, 1610, 1514, 1343, 1278, 1102 cm^{-1}; ^{1}H NMR (CDCl$_3$, 400 MHz) δ 2.36 (3H, s), 2.44 (3H, s), 2.95−2.98 (1H, m), 3.17−3.22 (1H, m), 4.55 (1H, dd, *J* = 1.6, 11.6 Hz), 4.63−4.87 (2H, m), 5.68−5.81 (1H, m), 6.58−6.59 (1H, m), 7.18 (2H, d, *J* = 7.2 Hz), 7.29 (2H, d, *J* = 6.8 Hz), 7.77 (2H, d, *J* = 7.6 Hz), 7.85 (2H, d, *J* = 7.2 Hz), 7.96 (2H, d, *J* = 7.2 Hz), 8.09 (1H, s), 8.20 (2H, d, *J* = 8.0 Hz); ^{13}C NMR (CDCl$_3$, 100 MHz) δ 21.8, 21.9, 38.9, 63.9, 74.6, 84.0, 89.4, 111.63, 118.88, 119.5, 126.2, 126.4, 126.7, 129.5, 129.8, 129.9, 132.7, 134.8, 144.5, 144.8, 146.4, 166.1, 166.2; ESI-TOF-MS *m/z* 565 [M + Na]$^+$; HRMS *m/z* calcd for C$_{29}$H$_{26}$N$_4$O$_7$Na ([M + Na]$^+$) 565.1699, found 565.1677.

1-[2′-Deoxy-3′,5′-bis{O-(p-toluoyl)}-β-D-ribofuranosyl]-4-(4-cyanophenyl)-1H-1,2,3-triazole (14). Using the general procedure, starting from 200 mg (0.506 mmol) of **5** and 77.199 mg (0.607 mmol) of 4-ethynylbenzonitrile (**D**), 237.84 mg (0.46 mmol) of compound **14** was isolated as a white solid: yield 90%; mp175−180 °C; IR (KBr) 2228, 1719, 1613, 1277, 1122 cm^{-1}; ^{1}H NMR (CDCl$_3$, 400 MHz) δ 2.28 (3H, s), 2.35 (3H, s), 2.83−2.89 (1H, m), 3.07−3.14 (1H, m), 4.46 (1H, dd, *J* = 4.0, 12.0 Hz), 4.61−4.63 (1H, m), 4.66 (1H, dd, *J* = 3.6, 12.0 Hz), 5.71−5.74 (m, 1H), 6.48 (1H, t, *J* = 6.4 Hz), 7.08 (2H, d, *J* = 8.0 Hz), 7.19 (2H, d, *J* = 7.6 Hz), 7.53 (2H, d, *J* = 8.4 Hz), 7.63 (2H, d, *J* = 8.4 Hz), 7.75 (2H, d, *J* = 8.0 Hz), 7.87 (2H, d, *J* = 8.0 Hz), 7.89 (1H, s); ^{13}C NMR (CDCl$_3$, 100 MHz) δ 21.8, 21.9, 38.9, 63.9, 74.6, 84.0, 89.4, 111.6, 118.9, 119.5, 126.2, 126.4, 126.7, 129.8, 130.0, 132.7, 134.8, 144.5, 144.8, 146.4, 166.1, 166.2; ESI-TOF-MS *m/z* 523 [M + H]$^+$; HRMS *m/z* calcd for C$_{30}$H$_{26}$N$_4$O$_5$Na ([M + Na]$^+$) 545.1801, found 545.1782.

General Procedure for Toluoyl Deprotection (1−4). The bistoluoylated triazolyl donor/acceptor nucleosides **11−14** (1 equiv) were dissolved in dry methanol. Sodium methoxide (3.5 equiv) was subsequently added. The solution was allowed to stir overnight at room temperature. The solution was evaporated, and the deprotected products were isolated pure by column chromatography (silica gel 60−120; pure EtOAc).

1-(2′-Deoxy-β-D-ribofuranosyl)-4-(phenanthren-9-yl)-1H-1,2,3-triazole (1). Using the general procedure for deprotection starting from 278.7 mg (0.467 mmol) of compound **11**, 155.2 mg (0.429 mmol) of compound **1** was isolated as a yellow solid: yield 92.0%; mp 166−168 °C; IR (KBr) 3364, 1435, 1205, 1121, 1056, 1032 cm^{-1}; ^{1}H NMR (CD$_3$OD, 400 MHz) δ 2.59−2.64 (1H, m), 2.91−2.96 (1H, m), 3.71 (1H, dd, *J* = 4.4, 11.6 Hz), 3.79−3.82 (1H, m), 4.08−4.1 (1H, m), 4.62−4.65 (1H, m), 6.57 (1H, t, *J* = 5.6, 6.0 Hz), 7.62−7.7 (4H, m), 7.96 (2H, d, *J* = 10.8 Hz), 8.25 (1H, d, *J* = 8.4 Hz), 8.57 (1H, s), 8.78−8.86 (2H, m); ^{13}C NMR (CD$_3$OD, 100 MHz) δ 42.1, 63.5, 72.5,

90.1, 90.8, 123.9, 124.3, 124.4, 127.4, 128.0, 128.3, 128.4, 128.8, 129.9, 130.2, 131.6, 132.1, 132.3, 132.9, 148.1; HRMS m/z calcd for $C_{21}H_{20}N_3O_3$ ([M + H]$^+$) 362.1499, found 362.1510.

1-(2′-Deoxy-β-D-ribofuranosyl)-4-(3,5-dimethoxyphenyl)-1H-1,2,3-triazole (2). Using the general procedure for deprotection starting from 290.9 mg (0.522 mmol) of compound **12**, 160.3 mg (0.499 mmol) of compound **2** was isolated as a white solid: yield 95.5%; mp 135−140 °C; IR (KBr) 3243, 1603, 1203, 1156, 1013 cm^{-1}; ^{1}H NMR (CD$_3$OD, 400 MHz) δ 2.51−2.57 (1H, m), 2.79−2.84 (1H, m), 3.66 (1H, dd, J = 4.8, 11.6 Hz), 3.73−3.75 (1H, m), 3.83 (6H, s), 4.03 (1H, q, J = 3.6 Hz), 4.58 (1H, q, J = 4.8, 4.4 Hz), 6.38−6.48 (m, 2H), 7.01 (1H, s), 8.54 (1H, s); ^{13}C NMR (CD$_3$OD, 100 MHz) δ 41.7, 55.9, 63.2, 72.2, 90.3, 101.5, 104.7, 121.1, 130.7, 133.3, 148.9, 162.8; HRMS m/z calcd for $C_{15}H_{20}$ N$_3$O$_5$ ([M + H]$^+$) 322.1393, found 322.1397.

1-(2′-Deoxy-β-D-ribofuranosyl)-4-(4-nitrophenyl)-1H-1,2,3-triazole (3). Using the general procedure for deprotection starting from 255.6 mg (0.472 mmol) of compound **13**, 132.05 mg (0.431 mmol) of compound **3** was isolated as a yellow solid: yield 91.43%; IR (KBr) 3526, 3265, 1606,1516, 1346, 1072 cm^{-1}; ^{1}H NMR (CD$_3$OD, 400 MHz) δ 2.54−2.58 (1H, m), 2.81−2.86 (1H, m), 3.67 (1H, dd, J = 4.8, 12.0 Hz), 3.77 (1H, dd, J = 4, 12.0 Hz), 4.06 (1H, q, J = 4.8 Hz), 4.58 (1H, q, J = 4.8 Hz), 6.48 (1H, t, J = 5.2, 6.4 Hz), 8.09 (2H, d, J = 8.8 Hz), 8.33 (2H, d, J = 9.2 Hz), 8.76 (1H, s); ^{13}C NMR (CD$_3$OD, 100 MHz) δ 61.3, 70.0, 88.1, 121.7, 124.1, 125.7, 136.7, 144.4, 145.4; HRMS m/z calcd for $C_{13}H_{14}N_4O_5Na$ ([M + Na]$^+$) 329.0856, found 329.0867.

1-(2′-Deoxy-β-D-ribofuranosyl)-4-(4-cyanophenyl)-1H-1,2,3-triazole (4). Using the general procedure for deprotection starting from 225 mg (0.431 mmol) of compound **14**, 111.92 mg (0.391 mmol) of compound **4** was isolated as a white solid: yield 90.8%; mp 142−145 °C; IR (KBr) 3243, 2230, 1359, 1167, 1100, 1063, 1037 cm^{-1}; ^{1}H NMR (CD$_3$OD, 400 MHz) δ 2.53−2.58 (1H, m), 2.79−2.85 (1H, m), 3.66 (1H, dd, J = 4.8, 12.0 Hz), 3.76 (1H, dd, J = 4.0, 12.4 Hz), 4.031−4.063 (1H, m), 4.56−4.62 (1H, m), 6.47 (1H, d, J = 5.6 Hz), 7.798 (2H, d, J = 8.4 Hz), 8.01 (2H, d, J = 8.4 Hz), 8.70 (1H, s); ^{13}C NMR (CD$_3$OD, 100 MHz) δ 41.9, 63.4, 72.3, 89.9, 90.6, 112.8, 119.8, 122.5, 127.4, 134.1, 136.5, 147.3; HRMS m/z calcd for $C_{14}H_{14}N_4O_3Na$ ([M + Na]$^+$) 309.0964, found 309.0969.

General Procedure for the Tritylation of 5′-OH (1a-DMTr, 3a-DMTr). A solution of **1** (99.34 mg, 0.275 mmol) or **3** (91.08 mg, 0.297 mmol) with 4-(dimethylamino)pyridine (catalytic amount) and 4,4′-dimethoxytrityl chloride (102.5 mg, 0.302 mmol and 110.7 mg, 0.326 mmol, respectively) in dry pyridine (3.0 mL) was stirred at room temperature for 16 h. After concentration of the solution to dryness, the residue was purified by silica gel column chromatography (CHCl$_3$:MeOH = 20:1) to yield the tritylated products (70%) as a pale yellow solid.

Data for 1-(5′-O-(4,4′-dimethoxytrityl)-2-deoxy-β-D-ribofuranosyl-4-(phenanthren-9-yl)-1H-1,2,3-triazole (1a-^{TPhen}B$_{Do}$-DMTr): ^{1}H NMR (CD$_3$OD, 300 MHz) δ 2.68 (1H, quintet, J = 6.9 Hz), 3.04−3.1 (1H, m), 3.49 (3H, s), 3.51 (3H, s), 4.06−4.19 (3H, m), 4.79−4.82 (1H, m), 6.61−6.67 (5H, m), 7.13−7.21 (7H, m), 7.32−7.40 (2H, m), 7.61−7.80 (5H, m), 8.04 (1H, d, J = 7.5 Hz), 8.44 (1H, s), 8.80 (2H, q, J = 9.0 Hz); ^{13}C NMR (CD$_3$OD, 75 MHz) δ 13.1, 40.3, 54.1, 63.2, 70.7, 86.4, 87.2, 89.2, 112.6, 122.3, 122.8, 125.9, 126.3, 126.6, 126.7, 127.1, 127.4, 128.1, 128.4, 128.7, 129.8, 129.9, 130.6, 131.2, 135.6, 140.8, 146.5,158.6; HRMS m/z calcd for $C_{42}H_{36}O_5N_3Na$ ([M + Na]$^+$) 686.2622, found 686.2626.

Data for 1-(5′-O-(4,4′-dimethoxytrityl)-2-deoxy-β-D-ribofuranosyl-4-(4-nitrophenyl)-1H-1,2,3-triazole (3a-^{TPhen}B$_{Ac}$-DMTr): ^{1}H NMR (CD$_3$OD, 300 MHz) δ 2.59−2.64 (3H, m), 2.94−3.01 (1H, m), 3.69 (6H, s), 4.13−4.16 (1H, m), 4.72 (1H, q, J = 6.0 Hz), 6.49 (1H, q, J = 6.0 Hz), 6.76 (4H, dd, J = 9.0 Hz), 7.24 (7H, dd, J = 2.4, 4.5 Hz), 7.36 (2H, d, J = 6.9 Hz), 7.75 (2H, d, J = 6.0 Hz), 8.2 (2H, d, J = 6.9 Hz), 8.63 (1H, s); ^{13}C NMR (CD$_3$OD, 300 MHz) δ 54.3, 63.3, 70.6, 86.4, 87.1, 89.2, 112.8, 121.3, 123.9, 125.9, 126.6, 127.5, 128.2, 129.9, 135.6, 135.7, 136.6, 144.5, 145.5, 147.3, 158.8. HRMS m/z calcd for $C_{34}H_{31}O_7N_4Na$ ([M + Na]$^+$) 631.2161 found 631.2157.

General Procedure for the Phosphoramidite Reaction (1a-^{TPhen}B$_{Do}$-Amidite, 3a-^{TNB}B$_{Ac}$-Amidite). To a solution of **1a** (39.78 mg, 0.060 mmol) or **3a** (36.48 mg, 0.060 mmol) and 1H-tetrazole in anhydrous acetonitrile (0.078 mmol) was added 2-cyanoethyl tetraisopropylphosphorodiamidite (24.8 μL, 0.078 mmol) under nitrogen. The reaction mixture was stirred at room temperature for 1 h. After completion of the reaction, the mixture was filtered off and immediately used for oligodeoxynucleotide synthesis without further purification.

General Procedure for Oligonucleotide Synthesis. All the reagents for DNA synthesis were purchased and used. ODNs were synthesized by a conventional phosphoramidite method by using an automated DNA/RNA synthesizer. ODNs were purified by reversed-phase HPLC on a 5-ODS-H column (10 × 150 mm, elution with 50 mM ammonium formate buffer (AF), pH 7.0, linear gradient over 45 min from 3% to 40% acetonitrile at a flow rate of 2.0 mL/min). The concentration of each ODN was determined from the molar extinction coefficient at 260 nm and 80 °C. Mass spectra of ODNs purified by HPLC were determined with a MALDI-TOF mass spectrometer.

Studies on the Photophysical Properties of the Nucleosides/Oligonucleotides. *UV−Vis Measurements.* All the UV−vis spectra of the nucleoside monomers (10 μM) were measured in different organic solvents using a UV−vis spectrophotometer with a cell of 1 cm path length at 25 °C. Equal volumes of each sample solution in different solvents were used. The measurements were taken in absorbance mode. The absorbance values of the sample solutions were measured in the wavelength regime of 200−550 nm. All the sample solutions were prepared just before the experiment was performed.

Fluorescence Experiments. All the sample solutions of the nucleoside monomers (10 μM) were prepared as described in UV measurement experiments. Fluorescence spectra were obtained using a fluorescence spectrophotometer at 25 °C and a 1 cm path length cell. The excitation wavelengths for the monomers were set at λ_{abs}^{max}, and emission spectra were measured in the wavelength regime of 315−600 nm with an integration time of 0.1 s. The fluorescence quantum yields (Φ$_f$) were determined using quinine sulfate as a reference with the known Φ$_f$ (0.54) in a 0.1 M solution in sulfuric acid.

UV−Vis and Thermal Melting Temperature (T_m) Measurements of the Oligonucleotides. All UV−vis spectra and T_m values of the ODNs (2.5 μM, final duplex concentration) were measured in 50 mM sodium phosphate buffers (pH 7.0) containing 100 mM sodium chloride. The measurements were taken in absorbance mode. The absorbance values of the sample solutions were measured in the wavelength regime of 200−500 nm. All the sample solutions were prepared just before the experiment was performed. A total volume of 120 μL from a stock solution of 700 μL of 2.5 μM concentration for each set was used for UV and T_m experiments in a microcell. Absorbance vs temperature profiles were measured at 260 nm using a UV−vis spectrophotometer equipped with a temperature controller using a 1 cm path length cell. The absorbance of the samples was monitored at 260 nm from 20 to 90 °C with a heating rate of 1 °C/min. From these profiles, the average method was used to determine the T_m values.

For the experiment related to the ground-state complexation phenomenon, the concentration of ODN **7** in 50 mM sodium phosphate buffers (pH 7.0) containing 100 mM sodium chloride was 15 μM.

Calculation of Thermodynamic Parameters. Thermodynamic parameters were determined by van't Hoff analysis using the relation $T_m^{-1} = R[\ln C_T]/\Delta H + \Delta S°/\Delta H°$, where $\Delta H°$ and $\Delta S°$ are the standard enthalpy and entropy changes determined from UV experiments, respectively, R is the universal gas constant, and C_T is the total strand concentration. From the slope of the plot of $1/T_m$ vs $\ln(C_T)$, ΔH was calculated, and then sustitution of this value into the value of the intercept yielded $\Delta S°$. Then we we were able to calculate ΔG. Thermodynamic parameters (25 °C) were determined from van't Hoff plots using at least four to five different concentrations for each duplex.

Fluorescence Experiments. ODN solutions were prepared as described for the UV−vis and T_m measurement experiments.

Fluorescence spectra were obtained using a fluorescence spectrophotometer at 25 °C using a 1 cm path length cell. The excitation wavelengths for single-strand duplex ODN were set at λ_{abs}^{max} (~307–340 nm), and emission spectra were measured in the wavelength regime of 300–600 nm with an integration time of 0.2 s. All the sample solutions were prepared just before the experiment was performed. A total volume of 500 μL from a stock solution of 700 μL of 2.5 μM concentration for each set was used for the fluorescence experiment in a 1 mL cell. The fluorescence quantum yields (Φ_f) were determined using quinine sulfate as a reference with the known Φ_f (0.54) in a 0.1 M solution in sulfuric acid.

For the fluorescence experiment at two temperatures and lifetime measurement experiment of ODN 7 and its hybrids with ODN 2, the concentration of ODN 7 was 15 μM in 50 mM sodium phosphate buffer (pH 7.0) containing 100 mM sodium chloride.

The fluorescence lifetime experiment was carried out using a time-resolved fluorescence spectrophotometer at 25 °C using a 1 cm path length cell. The concentration of ODN 7 was 15 μM, and those of ODN 2 were 0, 3, 6, 9, 12, and 15 μM. A 308 nm light-emitting diode (LED) was used as the excitation light source. The lifetime data were calculated by software with a fixed fitting range.

Circular Dichroism Measurement. CD experiments were performed with a CD spectropolarimeter equipped with a thermoelectric-type temperature control system (2.5 μM strand concentration, 50 mM sodium phosphate, 0.1 M sodium chloride, pH 7.0, room temperature). The data were collected using a 1 cm path length quartz cuvette with scanning from 380 to 200 nm, a time constant of 3 s, and a wavelength step size of 0.5 nm at 25 °C.

Theoretical Study. To get a preliminary idea about the charge transfer and the stacking propensity between two triazolyl donor/acceptor heteropairs/self-pairs or between natural nucleoside bases, without going for a rigorous theoretical calculation, we preliminarily calculated them using the Guassian 09[23] and ADF[21,22] program packages. A rigorous calculation will be done for other purposes, but at present the purpose of this is to support or to get an idea of the concept.

Thus, we have carried out a theoretical investigation on the charge transport property between triazolylphenanthrene as a donor and triazolylnitrobenzene as an acceptor with the ADF program package, which also showed a considerable amount of charge transfer characteristics.[21,22] A considerable amount of stacking interactions were also observed between the triazolylphenanthrene/triazolylnitrobenzene pair and pairs with natural nucleosides from DFT calculation using the M05-2X/6-31+G(d,p)[24] level of theory and Gaussian 09 program package.[23–25]

All the geometries of natural and unnatural bases were optimized by B3LYP/6-31+g(d,p), and stacked bases were optimized using the M05-2X density functional developed by Truhlar and Zhao.[24] The M05-2X functional is a hybrid meta-GGA (generalized gradient approximation) functional having 54% Hartree–Fock exchange contribution. Because of the large Hartree–Fock exchange contribution, this functional is a better choice than other functionals. This newly developed M05-2X functional has been found to be very suitable for studying a number of chemical problems and has especially been shown to be widely applicable to the study of noncovalent interactions. In the present preliminary calculation, the initial starting geometries of stacked dimer natural/unnatural hybrids in B-DNA conformation were generated using the macromodel program. From the generated structures in B-DNA conformation, we removed the sugar and phosphate backbone attached to the bases and satisfied all valences of all atoms with a hydrogen atom. In the case of the trimeric B-DNA duplex, the initial structure thus generated retains the B-DNA base conformation. We used the 6-31+G(d,p) basis set for geometry optimization to make these calculations feasible in the B-DNA conformation using the M05-2X density functional developed by Truhlar and Zhao.[24]

■ ASSOCIATED CONTENT

Ⓢ Supporting Information

Photophysical spectra, theoretical data, NMR spectra, and crystallographic data in CIF format. This material is available free of charge via the Internet at http://pubs.acs.org. The crystal structure for the nucleoside has been deposited at the Cambridge Crystallographic Data Centre with deposition number 873005 (http://www.ccdc.cam.ac.uk).

■ AUTHOR INFORMATION

Corresponding Author
*Phone: +91-361-2582324. Fax: +91-361-2582349. E-mail: ssbag75@iitg.ernet.in.

Notes
The authors declare no competing financial interest.

■ ACKNOWLEDGMENTS

■ REFERENCES

(1) (a) McLaughlin, L. W.; Wilson, M.; Ha, S. B. Use of Nucleoside Analogues To Probe Biochemical Processes. In *Comprehensive Natural Product Chemistry, Vol. 7, DNA and Aspects of Molecular Biology*; Barton, D. H. R., Nakanishi, K., Meth-Cohn, O., Eds.; Elsevier: New York, 1999; pp 252–284. (b) Kool, E. T.; Morales, J. C.; Guckian, K. M. *Angew. Chem., Int. Ed.* **2000**, *39*, 990. (c) Kool, E. T. *Acc. Chem. Res.* **2002**, *35*, 936. (d) Geyer, C. R.; Battersby, T. R.; Benner, S. A. *Structure* **2003**, *11*, 1485. (e) Benner, S. A. *Nature* **2003**, *421*, 118. (f) Benner, S. A.; Sismour, A. M. *Nat. Rev. Genet.* **2005**, *6*, 533. (g) Kimoto, M.; Cox, R. S., 3rd.; Hirao, I. *Expert Rev. Mol. Diagn.* **2011**, *3*, 321. (h) Hirao, I.; Kimoto, M.; Yamashige, R. *Acc. Chem. Res.* [Online early access]. DOI: 10.1021/ar200257x. Published Online: Jan 20, 2012. http://pubs.acs.org/doi/abs/10.1021%2Far200257x, accessed 11/4/2012.

(2) (a) Piccirilli, J. A.; Krauch, T.; Moroney, S. E.; Benner, S. A. *Nature* **1990**, *343*, 33. (b) Yang, Z.; Hutter, D.; Sheng, P.; Sismour, A. M.; Benner, S. A. *Nucleic Acids Res.* **2006**, *34*, 6095. (c) Hirao, I.; Kimoto, M.; Mitsui, T.; Fujiwara, T.; Kawai, R.; Sato, A.; Harada, Y.; Yokoyama, S. *Nat. Methods* **2006**, *3*, 729. (d) Doi, Y.; Chiba, J.; Morikawa, T.; Inouye, M. *J. Am. Chem. Soc.* **2008**, *130*, 8762. (e) Delaney, J. C.; Gao, J.; Liu, H.; Shrivastav, N.; Essigmann, J. M.; Kool, E. T. *Angew. Chem., Int. Ed.* **2009**, *48*, 4524. (f) Kim, H.-J.; Chen, F.; Benner, S. A. *J. Org. Chem.* **2012**, *77*, 3664.

(3) (a) Smith, S. A.; Rajur, S. B.; McLaughlin, L. W. *Nat. Struct. Biol.* **1994**, *1*, 198. (b) Lesser, D. R.; Kurpiewski, M. R.; Jen-Jacobson, L. *Science* **1990**, *250*, 776. (c) Kornberg, A.; Baker, T. A. *DNA Replication*, 2nd ed.; W. H. Freeman: New York, 1992. (d) Echols, H.; Goodman, M. F. *Annu. Rev. Biochem.* **1991**, *60*, 477. (e) Strazewski, P.; Tamm, C. *Angew. Chem., Int. Ed. Engl.* **1990**, *29*, 36. (f) Seo, Y. J.; Matsuda, S.; Romesberg, F. E. *J. Am. Chem. Soc.* **2009**, *131*, 5046. (g) Teo, Y. N.; Wilson, J. N.; Kool, E. T. *J. Am. Chem. Soc.* **2009**, *131*, 3923.

(4) (a) Kempe, T.; Sundquist, W. I.; Chow, F.; Hu, S. L. *Nucleic Acids Res.* **1985**, *13*, 45. (b) Zischler, H.; Nanda, I.; Schafer, R.; Schmid, M.; Epplen, J. T. *Hum. Genet.* **1989**, *82*, 227. (c) Hustedt, E. J.; Spaltenstein, A.; Kirchner, J. J.; Hopkins, P. B.; Robinson, B. H. *Biochemistry* **1993**, *32*, 1774. (d) Haugland, R. P. *The Handbook: A Guide to Fluorescent Probes and Labeling Technologies*; Molecular Probes: Carlsbad, CA, 2005. (e) Okamoto, A.; Saito, Y.; Saito, I. *J. Photochem. Photobiol., C* **2005**, *6*, 108. (f) Bag, S. S.; Kundu, R.; Matsumoto, K.; Saito, Y.; Saito, I. *Bioorg. Med. Chem. Lett.* **2010**, *20*, 3227. (g) Teo, Y. N.; Kool, E. T. *Chem. Rev.* **2012**, *112*, 4221.

(5) (a) Schweitzer, B. A.; Kool, E. T. *J. Am. Chem. Soc.* **1995**, *117*, 1863. (b) Kool, E. T. *Annu. Rev. Biochem.* **2002**, *71*, 191. (c) Seo, Y. J.; Matsuda, S.; Romesberg, F. E. *J. Am. Chem. Soc.* **2009**, *131*, 5046. (d) Jarchow-Choy, S. K.; Sjuvarsson, E.; Sintim, H. O.; Eriksson, S.; Kool, E. T. *J. Am. Chem. Soc.* **2009**, *131*, 5488. (e) Nakano, S.-i.; Fujii, M.; Sugimoto, N. *J. Nucleic Acids* [Online] **2011**, Article 967098. DOI: 10.4061/2011/967098. http://www.hindawi.com/journals/jna/2011/967098/, accessed 11/4/2012. (f) Chen, F.; Yang, Z.; Yan, M.; Alvarado, J. B.; Wang, G.; Benner, S. A. *Nucleic Acids Res.* **2011**, *39*, 3949. (g) Lavergne, T.; Malyshev, D. A.; Romesberg, F. E. *Chem.—Eur. J.* **2012**, *18*, 1231.

(6) (a) Wojciechowski, F.; Leumann, C. J. *Chem. Soc. Rev.* **2011**, *40*, 5669. (b) Grigorenko, N. A.; Leumann, C. J. *Chem.—Eur. J.* **2009**, *15*, 639. (c) Wilson, J. N.; Teo, Y. N.; Kool, E. T. *J. Am. Chem. Soc.* **2007**, *129*, 15426. (d) Robertson, N.; McGowan, C. A. *Chem. Soc. Rev.* **2003**, *32*, 96. (e) Keren, K.; Krueger, M.; Gilad, R.; Ben-Yoseph, G.; Sivan, U.; Braun, E. *Science* **2002**, *297*, 72. (f) Hall, D. B.; Holmlin, R. E.; Barton, J. K. *Nature* **1996**, *382*, 731.

(7) (a) Liu, J.; Cao, Z.; Lu, Y. *Chem. Rev.* **2009**, *109*, 1948. (b) Drummond, T. G.; Hill, M. G.; Barton, J. K. *Nat. Biotechnol.* **2003**, *21*, 1192. (c) Kolpashchikov, D. M.; Gerasimova, Y. V.; Khan, M. S. *ChemBioChem* **2011**, *12*, 2564. (d) Liu, L.; Li, Y.; Liotta, D.; Lutz, S. *Nucleic Acids Res.* **2009**, *37*, 4472.

(8) (a) Stambasky, J.; Hocek, M.; Kouovsky, P. *Chem. Rev.* **2009**, *109*, 6729 and references therein. (b) Kool, E. T. *Acc. Chem. Res.* **2002**, *35*, 936. (c) Tor, Y.; Dervan, P. B. *J. Am. Chem. Soc.* **1993**, *115*, 4461. (d) Clever, G. H.; Kaul, C.; Carell, T. *Angew. Chem., Int. Ed.* **2007**, *46*, 6226.

(9) (a) Rostovtsev, V. V.; Green, L. G.; Fokin, V. V.; Sharpless, K. B. *Angew. Chem., Int. Ed.* **2002**, *41*, 2596. (b) El-Sagheer, A. H.; Brown, T. *Chem. Soc. Rev.* **2010**, *39*, 1388. (c) Marks, I. S.; Kang, J. S.; Jones, B. T.; Landmark, K. J.; Cleland, A. J.; Taton, T. A. *Bioconjugate Chem.* **2011**, *22*, 1259. (d) Xiong, H.; Seela, F. *J. Org. Chem.* **2011**, *76*, 5584. (e) Xiong, H.; Leonard, P.; Seela, F. *Bioconjugate Chem.* **2012**, *23*, 856. (f) Sau, S. P.; Hrdlicka, P. J. *J. Org. Chem.* **2012**, *77*, 5.

(10) (a) Ren, R. X.-F.; Chaudhuri, N. C.; Paris, P. L.; Rumney, S., IV; Eric T. Kool, E. T. *J. Am. Chem. Soc.* **1996**, *118*, 7671. (b) Cahová, H.; Havran, L.; Brázdilová, P.; Pivoňková, H.; Pohl, R.; Fojta, M.; Hocek, M. *Angew. Chem., Int. Ed.* **2008**, *47*, 2059. (c) Amblard, F.; Cho, J. H.; Schinazi, R. F. *Chem. Rev.* **2009**, *109*, 4207.

(11) Bag, S. S.; Kundu, R. *J. Org. Chem.* **2011**, *76*, 3348.

(12) (a) Angell, Y. L.; Burgess, K. *Chem. Soc. Rev.* **2007**, *36*, 1674. (b) Moses, J. E.; Moorhouse, A. D. *Chem. Soc. Rev.* **2007**, *36*, 1249. (c) Tron, G. C.; Pirali, T.; Billington, R. A.; Canonico, P. L.; Sorba, G.; Genazzani, A. A. *Med. Res. Rev.* **2008**, *28*, 278. (d) Hein, C. D.; Liu, X.-M.; Wang, D. *Pharm. Res.* **2008**, *25*, 2216. (e) New, K.; Brechbiel, M. W. *Cancer Biother. Radiopharm.* **2009**, *24*, 289. (f) Frisch, B.; Hassane, F. S.; Schuber, F. *Methods Mol. Biol.* **2010**, *605*, 267. (g) Agalave, S. G.; Maujan, S. R.; Pore, V. S. *Chem.—Asian. J.* **2011**, *6*, 2696.

(13) Mulliken, R. S. *J. Am. Chem. Soc.* **1952**, *74*, 811.

(14) (a) Seidel, C. A. M.; Schulz, A.; Sauer, M. H. M. *J. Phys. Chem.* **1996**, *100*, 5541. (b) Poulin, K. W.; Smirnov, A. V.; Hawkins, M. E.; Balis, F. M.; Knutson, J. R. *Biochemistry* **2009**, *48*, 8861. (c) Wierzbinski, E.; de Leon, A.; Davis, K. L.; Bezer, S.; Wolak, M. A.; Kofke, M. J.; Schlaf, R.; Achim, C.; Waldeck, D. H. *Langmuir* **2012**, *28*, 1971. (d) Hervas, M.; Navarro, J. A.; De la Rosa, M. A. *Acc. Chem. Res.* **2003**, *36*, 798. (e) Berlin, Y. A.; Grozema, F. C.; Siebbeles, L. D. A.; Ratner, M. A. *J. Phys. Chem. C* **2008**, *112*, 10988.

(15) (a) Morrison, L. E.; Stols, L. M. *Biochemistry* **1993**, *32*, 3095. (b) Marras, S. A. E.; Kramer, F. R.; Tyagi, S. *Nucleic Acids Res.* **2002**, *30*, e122. (c) Li, Q.; Luan, G.; Guo, Q.; Liang, J. *Nucleic Acids Res.* **2002**, *30*, e5. (d) Nazarenko, I.; Pires, R.; Lowe, B.; Obaldy, M.; Rashtchian, A. *Nucleic Acids Res.* **2002**, *30*, 2089.

(16) (a) Johansson, M. K.; Fidder, H.; Dick, D.; Cook, R. M. *J. Am. Chem. Soc.* **2002**, *124*, 6950. (b) Eftink, M. R. Fluorescence Quenching: Theory and Applications. In *Topics in Fluorescence Spectroscopy*; Lakowicz, J. R., Ed.; Plenum Press: New York, 2002; Vol. 2, pp 53−126.

(17) (a) You, Y.; Tataurov, A. V.; Owczarzy, R. *Biopolymers* **2011**, *95*, 472. (b) Moreira, B. G.; You, Y.; Behlke, M. A.; Owczarzy, R. *Biochem. Biophys. Res. Commun.* **2005**, *327*, 473. (c) Kimoto, M.; Mitsui, T.; Yamashige, R.; Sato, A.; Yokoyama, S.; Hirao, I. *J. Am. Chem. Soc.* **2010**, *132*, 15418.

(18) (a) Bag, S. S.; Kundu, R.; Matsumoto, K.; Saito, Y.; Saito, I. *Bioorg. Med. Chem. Lett.* **2010**, *20*, 3227. (b) Sinkeldam, R. W.; Greco, N. J.; Tor, Y. *Chem. Rev.* **2010**, *110*, 2579.

(19) Chen, D.-W.; Beuscher, A. E., IV; Stevens, R. C.; Wirsching, P.; Lerner, R. A.; Janda, K. D. *J. Org. Chem.* **2001**, *66*, 1725.

(20) (a) Štimac, A.; Leban, I.; Kobe, J. *Synlett* **1999**, 1069. (b) Štimac, A.; Kobe, J. *Carbohydr. Res.* **2000**, *329*, 317. (c) Guezguez, R.; Bougrin, K.; Akri, K. E.; Benhida, R. *Tetrahedron Lett.* **2006**, *47*, 4807. (d) Chittepu, P.; Sirivolu, V. R.; Seela, F. *Bioorg. Med. Chem.* **2008**, *16*, 8427. (e) Malnuit, V.; Duca, M.; Manout, A.; Bougrin, K.; Benhida, R. *Synlett* **2009**, 2123. (f) Kolganova, N. A.; Florentiev, V. L.; Chudinov, A. V.; Zasedatelev, A. S.; Timofeev, E. N. *Chem. Biodiversity* **2011**, *8*, 568.

(21) (a) te Velde, G.; Bickelhaupt, F. M.; van Gisbergen, S. J. A.; Guerra, C. F.; Baerends, E. J.; Snijders, J. G.; Ziegler, T. *J. Comput. Chem.* **2001**, *22*, 931. (b) Guerra, C. F.; Snijders, J. G.; te Velde, G.; Baerends, E. J. *Theor. Chem. Acc.* **1998**, *99*, 391. (c) ADF2010, Scientific Computing and Modelling, Theoretical Chemistry, Vrije Universiteit, Amsterdam, The Netherlands, http://www.scm.com, accessed 7/6/2011.

(22) (a) Grimme, S. *J. Comput. Chem.* **2004**, *25*, 1463−1473. (b) Grimme, S. *J. Comput. Chem.* **2006**, *27*, 1787. (c) van der Wijst, T.; Lippert, B.; Swart, M.; Guerra, C. F.; Bickelhaupt, F. M. *J. Biol. Inorg. Chem.* **2010**, *15*, 387.

(23) Frisch, M. J.; Trucks, G. W.; Schlegel, H. B.; Scuseria, G. E.; Robb, M. A.; Cheeseman, J. R.; Montgomery, J. A., Jr.; Vreven, T.; Kudin, K. N.; Burant, J. C.; Millam, J. M.; Iyengar, S. S.; Tomasi, J.; Barone, V.; Mennucci, B.; Cossi, M.; Scalmani, G.; Rega, N.; Petersson, G. A.; Nakatsuji, H.; Hada, M.; Ehara, M.; Toyota, K.; Fukuda, R.; Hasegawa, J.; Ishida, M.; Nakajima, T.; Honda, Y.; Kitao, O.; Nakai, H.; Klene, M.; Li, X.; Knox, J. E.; Hratchian, H. P.; Cross, J. B.; Bakken, V.; Adamo, C.; Jaramillo, J.; Gomperts, R.; Stratmann, R. E.; Yazyev, O.; Austin, A. J.; Cammi, R.; Pomelli, C.; Ochterski, J. W.; Ayala, P. Y.; Morokuma, K.; Voth, G. A.; Salvador, P.; Dannenberg, J. J.; Zakrzewski, V. G.; Dapprich, S.; Daniels, A. D.; Strain, M. C.; Farkas, O.; Malick, D. K.; Rabuck, A. D.; Raghavachari, K.; Foresman, J. B.; Ortiz, J. V.; Cui, Q.; Baboul, A. G.; Clifford, S.; Cioslowski, J.; Stefanov, B. B.; Liu, G.; Liashenko, A.; Piskorz, P.; Komaromi, I.; Martin, R. L.; Fox, D. J.; Keith, T.; Al-Laham, M. A.; Peng, C. Y.; Nanayakkara, A.; Challacombe, M.; Gill, P. M. W.; Johnson, B.; Chen, W.; Wong, M. W.; Gonzalez, C.; Pople, J. A. *Gaussian 09*, revision A.1; Gaussian, Inc.: Wallingford, CT, 2009.

(24) (a) Zhao, Y.; Schultz, N. E.; Truhlar, D. G. *J. Chem. Theory Comput.* **2006**, *2*, 364. (b) Zhao, Y.; Truhlar, D. G. *Acc. Chem. Res.* **2008**, *41*, 157. (c) Zhao, Y.; Truhlar, D. G. *J. Chem. Phys.* **2006**, *125*, 194101. (d) Zhao, Y.; Truhlar, D. G. *J. Chem. Theory Comput.* **2007**, *3*, 289.

(25) Boys, S. F.; Bernardi, F. *Mol. Phys.* **1970**, *19*, 553.

(26) (a) Biegler König, F. W.; Schöbohm, J.; Bayles, D. *J. Comput. Chem.* **2001**, *22*, 545. (b) Robertazzi, A.; Platts, J. A. *J. Phys. Chem. A* **2006**, *110*, 3992.

(27) (a) Swart, M.; van der Wijst, T.; Guerra, C. F.; Bickelhaupt, F. M. *J. Mol. Model.* **2007**, *13*, 1245. (b) Gao, J. *Acc. Chem. Res.* **1996**, *29*, 298. (c) Monard, G.; Merz, K. M., Jr. *Acc. Chem. Res.* **1999**, *32*, 904. (d) Svensson, M.; Humbel, S.; Froese, R. D. J.; Matsubara, T.; Sieber, S.; Morokuma, K. *J. Phys. Chem.* **1996**, *100*, 19357. (e) Kosugi, T.; Hayashi, S. *J. Chem. Theory Comput.* **2012**, *8*, 322.

(28) (a) Zimmermann, N.; Meggers, E.; Schultz, P. G. *J. Am. Chem. Soc.* **2002**, *124*, 13684. (b) Atwell, S.; Meggers, E.; Spraggon, G.; Schultz, P. G. *J. Am. Chem. Soc.* **2001**, *123*, 12364. (c) Takezawa, Y.; Shionoya, M. *Acc. Chem. Res.* [Online early access]. DOI: 10.1021/ar200313h. Published Online: March 27, 2012. http://pubs.acs.org/doi/abs/10.1021%2Far200313h, accessed 11/4/2012.

(29) (a) Matsuda, S.; Fillo, J. D.; Henry, A. A.; Rai, P.; Wilkens, S. J.; Dwyer, T. J.; Geierstanger, B. H.; Wemmer, D. E.; Schultz, P. G.; Spraggon, G.; Romesberg, F. E. *J. Am. Chem. Soc.* **2007**, *129*, 10466. (b) Malyshev, D. A.; Pfaff, D. A.; Ippoliti, S. I.; Hwang, G. T.; Dwyer, T. J.; Romesberg, F. E. *Chemistry* **2010**, *16*, 12650. (d) Bugg, C. E. In *Solid-State Packing Patterns of Purine Bases*; Bergmann, E. D., Pullman, B., Eds.; The Israel Academy of Sciences and Humanities: Jerusalem, 1971; pp 178−204.

(30) (a) Loeb, L. A.; Preston, B. D. *Annu. Rev. Genet.* **1986**, *20*, 201. (b) Valis, L.; Amann, N.; Wagenknecht, H.-A. *Org. Biomol. Chem.* **2005**, *3*, 36. (c) Greco, N. J.; Tor, Y. *J. Am. Chem. Soc.* **2005**, *127*, 10784.

(31) (a) Berthet, N.; Constant, J. F.; Demeunynck, M.; Michon, P.; Lhomme, J. *J. Med. Chem.* **1997**, *40*, 3346. (b) Lhomme, J.; Constant, J. F.; Demeunynck, M. *Biopolymers* **1999**, *52*, 65. (c) Yoshimoto, K.; Nishizawa, S.; Minagawa, M.; Teramae, N. *J. Am. Chem. Soc.* **2003**, *125*, 8982.